Vol. 738: 161–185, 2024
https://doi.org/10.3354/meps14586

MARINE ECOLOGY PROGRESS SERIES
Mar Ecol Prog Ser

Published June 20

Thermal sensitivity of metabolic performance in *Squalus acanthias:* efficacy of aerobic scope as a predictor of viable thermal habitat

Alyssa M. Andres[1,6,*], Emily Slesinger[2,7], Rachael E. Young[2,8], Grace K. Saba[2], Vincent S. Saba[3,4], Beth A. Phelan[4], John Rosendale[4], Daniel Wieczorek[4], Connor F. White[5], Brad A. Seibel[1]

[1]University of South Florida, College of Marine Science, 830 1st St. S, St. Petersburg, FL 33701, USA
[2]Rutgers University, Institute of Marine and Coastal Sciences Building, 71 Dudley Rd., New Brunswick, NJ 08901, USA
[3]Princeton University, Geophysical Fluid Dynamics Laboratory, 201 Forrestal Road, Princeton, NJ 08540, USA
[4]Northeast Fisheries Science Center (NEFSC), National Marine Fisheries Service, National Oceanic and Atmospheric Administration, James J. Howard Marine Sciences Laboratory, 74 Magruder Road, Highlands, NJ 07732, USA
[5]Harvard University, Museum of Comparative Zoology Labs, 26 Oxford Street, Cambridge, MA 02138, USA
[6]*Present address:* Florida State University, Coastal and Marine Laboratory, 3618 Coastal Highway 98, St. Teresa, FL 32358, USA
[7]*Present address:* Alaska Fisheries Science Center, National Marine Fisheries Service, National Oceanic and Atmospheric Administration, Hatfield Marine Science Center, 2030 SE Marine Science Dr., Newport, OR 97365, USA
[8]*Present address:* Rowan University, 201 Mullica Hill Rd., Glassboro, NJ 08028, USA

ABSTRACT: Ocean warming due to climate change can affect the metabolism, performance, and survival of ectothermic marine species. On the US Northeast continental shelf (US NES), waters are warming faster than the global average, leading to elevated mean temperatures and an increased risk of marine heatwave exposure in the region. Thus, it is critical to understand the effects of warming on the region's living marine resources. Here, we quantified the acute temperature sensitivity of metabolic traits to evaluate their role as possible drivers of acute thermal tolerance and viable habitat in the spiny dogfish shark *Squalus acanthias* on the US NES. From 10–23°C, the standard metabolic rate increased more rapidly than the maximum metabolic rate, resulting in a reduction in factorial aerobic scope at warmer temperatures. However, the oxygen supply capacity increased with temperature in proportion to maximum metabolic rate, and neither metric declined at the warmest temperatures, suggesting oxygen supply capacity does not limit performance within the tested range. Although behavioral observations revealed overt thermal stress via loss of equilibrium at ⩾20°C and estimated lethal temperature at ~24°C, sharks retained the ability to regulate their resting metabolic rate, achieve maximum activity, and peak absolute aerobic scope at warm temperatures. Results suggest that factors other than oxygen supply or aerobic scope are constraining thermal tolerance in *S. acanthias* and support the notion that aerobic scope cannot be universally applied to determine optimal or viable metabolic habitat.

KEY WORDS: Elasmobranch · Aerobic scope · Thermal tolerance · Climate change · Metabolism

1. INTRODUCTION

The temperature sensitivities of oxygen supply and demand are hypothesized to play a role in dictating viable species habitat for marine ectotherms (e.g. Pörtner 2010, Deutsch et al. 2015, 2020, Seibel & Birk 2022, Somero 2022). On the US Northeast Continental Shelf (US NES), mean surface and bottom temperatures are expected to increase by ~3.7–5°C by century's end, a rate of warming 2–3× faster than the

*Corresponding author: ama23f@fsu.edu

global average (Pershing et al. 2015, Saba et al. 2016, Kleisner et al. 2017, Caesar et al. 2018), elevating concern for resident marine species. As one of the most rapidly warming regions in the world (Wu et al. 2012, Forsyth et al. 2015), the US NES carries an additional increased risk of acute heating events that are largely driven by increases in sea surface temperature (Oliver et al. 2019). Defined as prolonged (>5 d) extreme anomalous heating events exceeding the 90th percentile of seasonally varying climatology (Hobday et al. 2016), surface and subsurface marine heatwaves have increased in frequency (34%) and duration (17%) globally in the last century (Oliver et al. 2018, 2021) and are projected to increase indefinitely under climate change (Frölicher et al. 2018, Oliver et al. 2021). As acute and long-term rising temperatures threaten survival or decreased fitness, many key species in the region have exhibited poleward shifts in distribution or movement to deeper water in step with local climate warming (Friedland & Hare 2007, Nye et al. 2009, Hazen et al. 2013, Pinsky et al. 2013, Kavanaugh et al. 2017, Kleisner et al. 2017, Morley et al. 2018, Rogers et al. 2020). Such biogeographical changes have the potential to profoundly impact ecosystem dynamics and resource management; however, there are large gaps in our understanding of species' acute and long-term thermal tolerances and the degree to which such tolerances may drive climate-induced shifts in biogeography. By identifying underlying physiological drivers of thermal tolerance and evaluating physiological parameters as indicators of optimal and viable habitat, we may add clarity in predicting the responses of species to ocean warming.

Evaluating thermal sensitivity of metabolic parameters reveals changes in organism performance and energetic needs across a species' thermal range. In particular, the scope for aerobic performance is an indicator of the total energy available to support aerobic processes, such as foraging, growth, and reproduction, which are critical for fitness. Aerobic scope is measured as the factorial (FAS) or absolute (AAS) difference between maximum (MMR, active) and standard (SMR, resting) metabolic rates and allows us to quantify the proportional and absolute increases in oxygen consumption above basic demands that an animal can achieve (Clark et al. 2013). SMR typically demonstrates greater thermal sensitivity and increases faster with temperature than MMR (Killen et al. 2017, Seibel & Deutsch 2020, Seibel & Birk 2022). As a result, the scope of available energy changes across temperature; FAS (MMR/SMR) tends to decline with increasing temperature toward critical values that may constrain biogeography (Deutsch et al. 2020). By contrast, AAS (MMR − SMR) increases with temperature, often to a peak with a subsequent decline along a bell-shaped curve. The peak in AAS is typically interpreted as an optimum temperature, one that wild populations are thought to actively seek out to optimize fitness, while the decrement at higher temperatures is often attributed to a declining ability to supply oxygen to tissues in support of elevated demands at high temperature (Fry 1971, Pörtner 2010, Clark et al. 2013, Rubalcaba et al. 2020). The temperature at which AAS declines significantly from its peak in warm water has previously been used to identify population limits below lethal temperatures. However, such thermal trends in AAS are species-specific, lack universality, and their interpretations have seldom been tested mechanistically (Schulte 2015, Lefevre 2016, Jutfelt et al. 2018). For example, the shape of the thermal trend in AAS deviates from the typical bell curve for many species and may present, with either a left or right shift in the curve, as either a very broad-scope curve (increase of SMR and MMR in parallel up to temperatures close to maximum) or increase up to lethal limits accompanied by a rapid decline as death proceeds (Fry 1947, Clark 2006, Healy & Schulte 2012, Schulte 2015), with no clear connection between the aerobic scope curve and temperatures that may maximize different fitness-related traits (e.g. Healy & Schulte 2012, Norin et al. 2014). Furthermore, oxygen supply capacity (α), a measure of an animal's maximum ability to supply oxygen to respiring tissues, which encompasses all physiological processes involved in supplying oxygen to the body (e.g. ventilation, circulation, diffusion, blood oxygen carrying capacity), can be directly determined from metabolic measurements. Directly measuring this metric provides an opportunity to test whether oxygen supply is a cause of the declining performance observed at temperature extremes (Seibel & Deutsch 2020). Thus, the balance between thermally sensitive energetic demands and oxygen supply may constrain aerobic scope as well as thermal tolerance, and metabolic traits may be used to model viable species habitat (e.g. Pörtner 2010, Deutsch et al. 2020, Seibel & Birk 2022).

For the spiny dogfish shark *Squalus acanthias*, a small benthopelagic shark (maximum total length range: 110–130 cm) representing the most abundant elasmobranch within the Northwest Atlantic, spatiotemporal responses to warming conditions have been unclear. *S. acanthias* has been regarded as a keystone species, a key ecosystem modifier in the region (Morgan & Sulikowski 2015), and one of the most dominant piscivores on the US NES (Link & Garrison 2002, Rafferty et al. 2012, Morgan & Sulikowski 2015), rapidly filling ecosystem niches vacated by heavily overfished resources. In addition, *S. acanthias* is a valuable commercial resource, with landings in the Western North Atlantic totaling more than 7575 metric tons (17 million lbs) in 2020 valued at ~$3.2 million US (NEFSC 2006). Shifts in *S. acanthias* distribution and abundance under climate change and acute heating events may have wide-ranging ecological consequences and implications for the management of this species. As such, it is critical to investigate the dynamics of this species in the region and develop tools beyond ecological surveys to predict thermal tolerances and potential shifts in viable habitat for *S. acanthias* in the face of rising ocean temperatures and the increased incidence of acute marine heating events.

S. acanthias is a wide-ranging species, found in North American continental shelf waters from Florida to Labrador, most commonly from Cape Hatteras, NC, to Nova Scotia (Burgess 2002). These sharks are detected most often at depths of 50–150 m (range: surface to >500 m; Compagno 1984, Compagno et al. 2005, Stehlik 2007, Castro & Peebles 2011) and are most frequently captured at low temperatures ~6–15°C (Compagno 1984). *S. acanthias* populations generally avoid temperatures >23°C (Carlson et al. 2014) and migrate latitudinally and offshore on a seasonal basis, coincident with bottom temperature changes (Templeman 1984, Rago et al. 1998, Stehlik 2007, Ulrich et al. 2007, Sagarese et al. 2014). However, studies of *in situ* movement conducted on satellite-tagged *S. acanthias* have revealed clear differences in seasonal distributions, length of seasonal residencies, magnitude of north–south and inshore–offshore seasonal migrations, and thermal associations between northern and southern portions of the stock (Carlson et al. 2014), lending support to the idea that there are subpopulations that may differ in thermal habitat use and potentially thermal tolerance across the species' range. Physiological tolerance thresholds and thermal sensitivities for this species remain unknown, as are the energetic needs and specific metabolic responses to temperature across the species' distribution.

This study investigated the acute temperature sensitivity of metabolic traits in *S. acanthias* of the mid-Atlantic US NES, evaluating potential drivers of acute thermal tolerance and the utility of aerobic scope in predicting optimal and sublethal limiting thermal conditions for this species. We mechanistically tested the role of oxygen supply in temperature-limitation (Seibel & Deutsch 2020). We hypothesized (Fig. S1 in the Supplement at www.int-res.com/articles/suppl/m738p161_supp.pdf) that for *S. acanthias*, AAS would peak at an 'optimal' temperature corresponding to the preferred thermal habitat of wild *S. acanthias* within the study region. We hypothesized that a significant decline in aerobic scope beyond its peak, caused by a breakdown in physiological oxygen supply and performance, would coincide with a sublethal warm temperature limit approaching 23°C. We expected that FAS would demonstrate an inverse relationship with temperature for *S. acanthias* and would decline to a minimum limiting threshold near 3 (Deutsch et al. 2020) at 23°C for this population. Results from this study serve to clarify our understanding of the drivers of acute thermal tolerance and energetic performance in *S. acanthias* and contribute to evaluating metabolic metrics as indicators of viable habitat, particularly relevant in an era of increasing thermal volatility.

2. MATERIALS AND METHODS

2.1. Animal collection and care

Adult *Squalus acanthias* (n = 90) were collected via gillnet (depth: 35–50 ft [~11–15 m]; temperature: 11.7°C) off Long Beach Island, NJ, in November and December 2016 and 2017 (Captain Kevin Wark, FV 'Dana Christine', Barnegat, New Jersey). Animals were transported to NOAA's James J. Howard Sandy Hook Marine Laboratory in Highlands, NJ, and held in designated circular holding tanks (1601–2846 l; 2–8 ind. tank^{-1} depending on tank volume) at ambient temperature (~7–13°C). Holding tanks were connected to a flow-through system supplied with filtered and UV-treated water drawn from the bayside of Sandy Hook. Subjects were held in captivity for 2–3 wk prior to experimentation, maintained on a diet of herring *Clupea harengus*, butterfish *Peprilus triacanthus*, and silversides *Menidia menidia*, and fed ad libitum every other day. Sharks were measured for length (Table 1) and ID-tagged via color-coded T-bar tags (second dorsal fin).

2.2. Ethics statement

Captive animal husbandry was conducted under veterinary guidelines and procedures approved by the Institutional Animal Care and Use Committee at Rutgers University (protocol no. 15054).

Table 1. *Squalus acanthias* demographics and trial summaries. Reported as means ± SD

	Temperature bin (°C)				
	10	13	17	21	23
Intermittent respirometry cycle (cycle phase lengths in min:s) range and (mode)					
Flush	3–6 (6)	6–8 (6)	7–11 (7)	10–12 (12)	12–14 (12)
Wait	1	1	1	1	1
Measure	8–12 (10)	6–8:30	6–7:30 (7.5)	5–6 (5)	4–5 (5)
Maximum metabolic rate trials					
n	22	17	21	23	21
n (for α)	22	17	21	27	21
Sex ratio (F:M)	14:8	9:8	16:5	15:8	17:4
Mean temp (°C)	10.14 ± 0.5	13.35 ± 0.36	17.11 ± 1.03	21.24 ± 0.35	23.12 ± 0.38
Precaudal length (cm)	67.1 ± 5.16	66.59 ± 5.36	68.15 ± 5.82	68.43 ± 5.13	69.98 ± 6.41
Fork length (cm)	73.85 ± 5.77	72.59 ± 4.99	74.70 ± 6.32	75.19 ± 5.99	76.89 ± 5.59
Stretch total length (cm)	83.28 ± 6.29	81.89 ± 5.61	84.47 ± 6.78	84.36 ± 5.70	86.3 ± 5.82
Mass (kg)	2.3 ± 0.84	2.13 ± 0.75	2.21 ± 0.67	2.26 ± 0.61	2.32 ± 0.63
PO_2 at MMR (kPa)	20.09 ± 1.25	19.07 ± 1.39	18.81 ± 1.32	17.6 ± 1.41	17.65 ± 1.37
Max. trial PO_2 (kPa)	21 ± 0.63	20.4 ± 0.64	20.18 ± 0.55	19.75 ± 0.64	19.44 ± 0.69
Min. trial PO_2 (kPa)	19.28 ± 0.85	17.06 ± 2.01	17.57 ± 0.82	16.57 ± 1.18	16.19 ± 1.35
Hypoxia trials					
n	8	7	6	8	6
Sex ratio (F:M)	4:4	3:4	4:2	4:4	4:2
Mean temp (°C)	9.64 ± 0.1	13.5 ± 0.01	16.9 ± 0.72	20.44 ± 0.56	22.19 ± 002
Precaudal length (cm)	64.19 ± 2.8	64.92 ± 3.97	70.8 ± 6.02	65.25 ± 2.63	67.1 ± 4.53
Fork length (cm)	70.5 ± 3.22	71.25 ± 4.13	77.4 ± 6.64	71.69 ± 2.74	73.67 ± 5.14
Stretch total length (cm)	79.91 ± 3.73	80.58 ± 4.68	87.8 ± 7.42	81.23 ± 3.08	83.12 ± 5.51
Mass (kg)	1.89 ± 0.31	1.87 ± 0.57	2.15 ± 0.68	1.86 ± 0.27	2 ± 0.56

2.3. Trial group selection

Following the 2–3 wk captive adjustment period, *S. acanthias* individuals that fed regularly and expressed no overt illness or behavioral abnormalities were included in physiological measurements (n = 71). Physiological metrics were measured at a total of 5 experimental target temperatures (10, 13, 17, 21, and 23°C). Power analyses conducted using the results of previous research on thermal and oxygen sensitivity of black seabass *Centropristis striata* (Slesinger et al. 2019) were used to guide sample size determination across trials. A total of 24 individuals were assigned to each experimental temperature group. For trial group selection, animals were sorted by sex and selected for temperature groups at random from each of the sexes, with the aim of achieving close to a ~50% ratio of males to females for each experimental temperature.

To obtain metabolic performance metrics at each experimental temperature, *S. acanthias* were subjected to 2 distinct metabolic challenges (described in detail below): (1) maximum exercise (exercise trial protocol) and (2) hypoxia (hypoxic trial protocol). A flow diagram of thermal testing is detailed in Fig. S2. In Year 1, thermal experiments were run sequentially from low to high temperatures. In Year 2, the order of the first 4 experimental temperatures (10–21°C) was randomized to allow for greater testing of 'new individuals' (individuals that had not undergone testing yet) across temperature groups (see Fig. S2). In both years, the highest temperature, 23°C, was conducted last in order to avoid thermal stress-related effects on measurements at other temperatures. Due to subject attrition (ca. 31% total) and limited access to further animal collection, 'recovered' sharks (in good condition) were included in subsequent temperature trials after recovering for a minimum of 6 d following their most recent trial and resumed feeding behavior. Individuals were used only once per target temperature and a maximum of 3 target temperatures.

2.4. Experimental setup

To understand how energetic demands change across the *S. acanthias* thermal range, temperature-controlled intermittent respirometry (Clark et al. 2013, Svendsen et al. 2016) was used to measure the rates of oxygen consumption as a proxy for metabolic rate. The 3-phase intermittent respirometry cycle included, in sequence, (1) a closed-chamber 'measure' period in which the decline in dissolved oxygen (DO) within the chamber was recorded; (2) an open-chamber 'flush' period that allowed for refreshment of oxygen and removal of accumulated metabolic waste; and (3) a closed-chamber 'wait' period that allowed uniform mixing and equilibration of oxygen before measurement. The duration of cycle phases was temperature-dependent (due to the solubility of oxygen decreasing in warmer waters and DO depletion occurring at a much higher rate at warm temperatures due to elevated organism demands) and initially calibrated to reach starting oxygen levels (air saturation) by the end of a flush period (Table 1). Intermittent respirometry phases were automated using a DAQ-M instrument (Loligo Systems) for exercise trials but were controlled manually during hypoxia trials.

Experiments were conducted in twin 8000 l recirculating aquaculture systems. Each of these systems consisted of a sand filter (50 µm pore size; Arias 8000 sand filter), UV filtration (Twin Smart UV-High-Output Sterilizer), activated carbon (Clean & Clear Cartridge Filter), and biologic filtration using a bioreactor (Sweetwater Low-Space Bioreactor). The system included a combination of water sourced from Sandy Hook Bay and sea salt (Aquavitro) to maintain salinity (mean ± SD: 31.98 ± 0.76). The experimental setup (Fig. 1) allowed for simultaneous testing of 4 individuals. Each shark was enclosed within an acrylic respirometry chamber (100 × 32.5 × 32.5 cm, 106.69 l; inclusive of tubing volume; average chamber volume to animal volume ratio: 44.45), submerged in 2 round tanks containing aerated seawater (1.83 m diameter; 1200.96 l; 2 chambers per temperature bath) that served as temperature control and replenishment water during flush periods (Fig. 1). A recirculation pump (Eheim Universal 2400 l h^{-1}) was affixed to each chamber in a closed loop (via gas impermeable Tygon® tubing) and provided continuous mixing in the respirometer. A second pump (i.e. flush pump; Eheim Universal 1200 l h^{-1}) was used in an open circuit to supply aerated seawater during flush periods. A 1-way valve at the posterior end of each chamber permitted outflow of water during flushes. DO concentration within each chamber was measured using an oxygen dipping probe optical mini sensor (PreSens PSt3), placed within the closed recirculation loop and connected to a multichannel oxygen meter (Witrox-4 instrument, Loligo Systems). A temperature probe (Loligo Systems Pt1000) within the seawater bath allowed for continuous temperature monitoring. Oxygen and temperature were sampled at a rate of 1 Hz for the duration of each trial using Loligo Systems AutoResp Software. Temperature was maintained at ±1°C of the starting temperature using in-line combination heater–chillers (Aqua Logic Delta Star) and closed-cell foam insulation (5.08 cm) surrounding tanks. To minimize disturbance to the sharks during trials, experimental tanks were covered with insulated foam lids, with a small built-in window to maintain photoperiod.

2.5. Exercise trial protocol

To obtain measures of MMR, α, and measures of resting metabolic rates (RMR and SMR), *S. acanthias* (n = 24 per experimental temperature) underwent a 22 h intermittent respirometry exercise trial. Prior to testing, subjects were held at the designated experi-

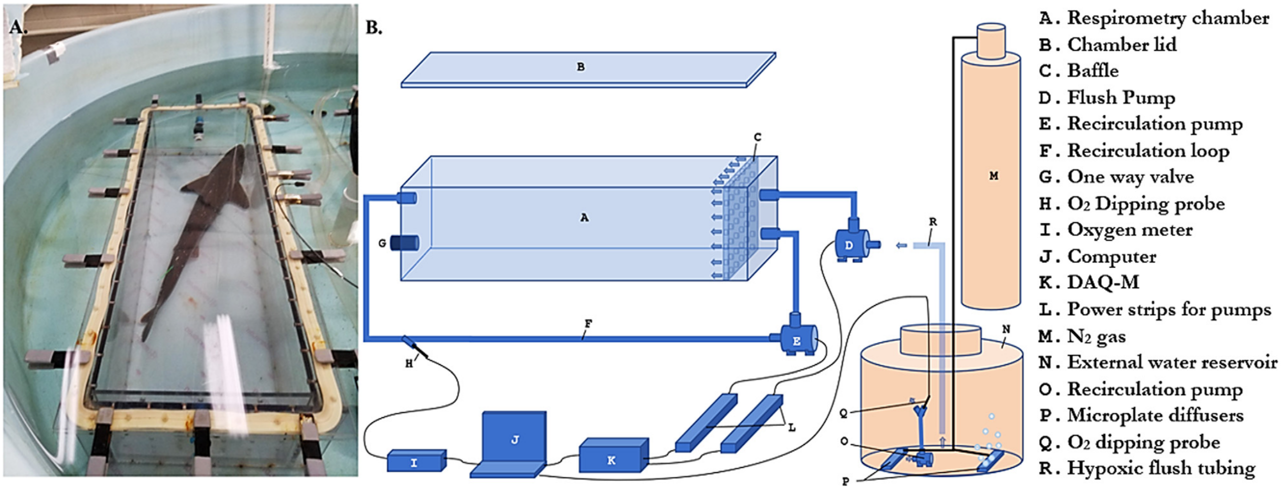

Fig. 1. (A) *Squalus acanthias* sealed within an intermittent respirometry chamber, submerged in the temperature bath. (B) Experimental setup with equipment labels corresponding to names on the right. Items A–H were fully submerged within the temperature bath for the duration of trials. Items M–R were used in hypoxic trials only. Blue arrows indicate direction of water flow

mental temperature for a 48 h acute acclimation period, following a thermal adjustment from holding temperature ($\pm 3°C\ d^{-1}$). Subjects were fasted 72 h prior to metabolic testing to eliminate postprandial metabolism (Ferry-Graham & Gibb 2001, Chabot et al. 2016a). To begin the experiment, *S. acanthias* were individually weighed and placed in a separate 'chase' tank (diameter: 1.83 m; 1200 l). Individuals were then exercised to exhaustion via tactile stimulation to elicit MMR (Clark et al. 2013, Rummer et al. 2016, Killen et al. 2017). Exhaustion was quantified by the subject's lack of response to both tactile stimulation and brief air exposure. The sharks were then sealed within the experimental chambers for immediate respirometry measurement as described above. Start times for individuals within a trial group were by necessity staggered to accommodate individual exercise prior to immediate measurement of MMR; however, all individual start times occurred within a 1.5 h time frame, beginning at the same time of day. Once measurement began, subjects were allowed to recover in the chambers and return to RMR over the 22 h time frame of the trial. The time frame of experimentation encompassed the MMR after exercise and subsequent recovery to RMRs. At the end of the 22 h exercise trials, 14 individuals from each temperature were removed from the chambers to recover, while a subset of 8 individuals in Year 2 remained within the chamber for further testing under hypoxic conditions.

2.6. Hypoxia trial protocol

To obtain measures of α (independent of MMR), to confirm SMR (lowest RMRs), and to determine the critical oxygen level that limits SMR (P_{cSMR}), we investigated changes in metabolism under interacting temperature and oxygen conditions. For hypoxia trials, 8 individuals at each temperature remained in the experimental chambers following their 22 h exercise protocol to undergo intermittent respirometry testing under declining oxygen conditions. Start times were standardized to the same time of day. Intermittent respirometry was used as previously described, but during flush periods of the hypoxia trial, DO was manually reduced by the addition of low O_2 water from an external reservoir (Fig. 1). Ceramic plate micro-oxygen diffusers (Point Four™) were used to disperse N_2 gas and displace DO in the reservoir by ~10% before each flush (Rogers et al. 2016, Snyder et al. 2016). DO within the reservoir was monitored using an additional oxygen dipping probe optical mini sensor (PreSens PSt3) connected to the Witrox-4 instrument (Loligo Systems) with manual control of N_2 gas. Hypoxia trials progressed until P_{cSMR} was reliably reached, indicated by a stark and continuous decline in an individual's metabolic rate that fell below normal resting measures for each individual. The P_{cSMR} threshold represents the oxygen level at which an animal can no longer maintain their SMR independent of environmental oxygen, where aerobic scope is functionally zero, and survival becomes time-limited. At P_{cSMR}, organisms also reliably operate at maximum α (Seibel et al. 2021). Upon reaching P_{cSMR} and the conclusion of the hypoxia trial, individuals were then removed from the chamber to recover overnight at full air saturation.

2.7. Background respiration

To account for microbial respiration in chambers during experimentation, background O_2 consumption was determined over a continuous 2 h, closed-chamber period following the removal of *S. acanthias* from experimental chambers after metabolic testing. The background mass-specific rate of oxygen consumption (MO_2) was obtained independently in each experimental chamber, after each individual trail, at each experimental temperature. Background MO_2 was then calculated for each trial and chamber as the mean MO_2 of all measure periods within the 2 h background trial. Individual background MO_2 was then subtracted from the MO_2 measures of the *S. acanthias* trial from which they were derived. To minimize microbial growth throughout testing, respirometers were scrubbed and rinsed with fresh water once a week and air-dried before reassembly.

2.8. Metabolic rate (MO_2) and metabolic trait calculations

A summary of metabolic definitions, acronyms, and the source of each measured metric is listed in Table 2. MO_2 was calculated for each measure period using Eq. (1):

$$MO_2 = \frac{(S - \mathrm{br}) \times V}{M} \tag{1}$$

where MO_2 is measured in mg O_2 kg^{-1} h^{-1}, S is the slope of the linear regression of MO_2 vs. time (mg O_2 l^{-1} h^{-1}), V is the total volume (l) of the respirometry chamber minus the volume of the animal, br is the mean background microbial O_2 consumption rate (mg O_2 l^{-1} h^{-1}), and M is the mass of the individual

Table 2. Metabolic trait definitions, methods, and associated equations for *Squalus acanthias* trials. MO_2: mass specific metabolic rate; $q_{0.2}$: 20th quantile of the lowest normal distribution of MO_2; PO_2: oxygen partial pressure; A: theoretical upper horizontal asymptote of the thermal curve; B: temperature value at the inflection point of the logistic curve; C: scaling parameter indicating the steepness of the increase in metabolic rate with temperature; k_B: Boltzmanns constant; T: absolute temperature in Kelvin

Metric	Name and definition of metric	Measured and/ or modeled	Defined by	Source trial	Associated equation or modeled equation
SMR	Standard metabolic rate; lowest metabolic rate supporting basal metabolism of conscious shark at rest	Measured (limited), modeled	$q_{0.2}$ of MO_2 values prior to oxygen limitation	Hypoxia	Modeled: $f(x) = e^x$
P_c	Critical (limiting) O_2 partial pressure for a given metabolic rate across the activity spectrum (e.g. P_{cSMR}: critical O_2 for SMR; P_{cMAX}: critical O_2 for MMR at 21 kPa)	Measured (limited), modeled	α, MO_2, PO_2 (α-method; Seibel et al. 2021)	Both	$P_c = MO_2/\alpha$ e.g. $P_{cSMR} = SMR/\alpha$
MMR (measured)	Highest metabolic rate achieved in trials	Measured, modeled	Highest MO_2 value in trial	Maximum metabolic rate	Modeled: $y = \dfrac{A}{1 + \exp^{\frac{(B-x)}{C}}}$
Predicted MMR (at 21 kPa)	Predicted maximum metabolic rate at air saturation (MMR = $\alpha \times P_{cMAX}$ of 21 kPa)	Modeled	SMR, P_{cSMR}, and/or α, P_{cMAX} =21 kPa	Both	$MMR = \alpha \times P_{cMAX}$ $(MMR = \alpha \times 21)$
AAS	Absolute aerobic scope (modeled and calculated using population mean MMR and SMR values)	Measured, modeled	MMR (at 21 kPa), MMR, SMR	Both	AAS = MMR−SMR
FAS	Factorial aerobic scope (modeled and calculated using population mean MMR and SMR values)	Measured, modeled	MMR (predicted at 21 kPa), MMR, SMR	Both	FAS = MMR/SMR
α	Physiological oxygen supply capacity (maximum measured value of physio logical oxygen supply; α_0)	Measured, modeled	Maximum value of α_0 (instantaneous oxygen supply) in trial	Both	Highest value of $\alpha_0 = MO_2 / PO_2$ Modeled: $y = \dfrac{A}{1 + \exp^{\frac{(B-x)}{C}}}$
α-line	Linear relationship of critical O_2 partial pressure across activity	Modeled	α = slope of α-line ($\alpha = MO_2 / P_c$ for given MO_2), intercept = (0,0), P_{cMAX}	Both	$y = \alpha \times x$ $MO_2 = \alpha \times PO_2$
Chase time	Length of chase exercise to 'exhaustion'	Measured	Time to exhaustion (s)	Maximum metabolic rate	NA
Q_{10}	The factorial change in a metabolic metric for a 10°C change in temperature. Indication of temperature sensitivity, (higher values = more temperature sensitive)	Measured	Metabolic rates (R_1, R_2) at 2 distinct temperatures (T_1, T_2)	Both	$Q_{10} = \left(\dfrac{R_2}{R_1}\right)^{\left(\frac{10}{T_2 - T_1}\right)}$
E	Activation energy of metabolism. The minimum amount of energy required for metabolic reactions to occur. Indication of temperature sensitivity	Measured	Slope of linear regression of Arrhenius plots	Both	$\text{Ln(metric)} = E \times (1 / k_B T) + b$

S. acanthias (kg). Measure periods that showed a linear regression with $R^2 < 0.75$ were excluded from the data sets (Killen et al. 2021).

In this study, MMR was defined as the maximum MO_2 measured. Measures of RMR within the exercise trials were calculated as the quantile at $p = 0.2$, ($q_{0.2}$) of all MO_2 measures (Claireaux & Chabot 2016) after the first 5 h of exercise trials. Measures of RMR were used for comparison with measures of RMRs within the hypoxia trials that were defined as SMR (RMRs in hypoxia trials). Measures of SMR were calculated as the quantile at $p = 0.2$ ($q_{0.2}$) of all MO_2 measures prior to oxygen limitation within hypoxia trials. Oxygen limitation in hypoxia trials was indicated by a decline in MO_2 below the lowest consistent resting measures. Quantiles were chosen to account for any sporadic activity in experimental chambers that could not be directly observed or quantified, minimizing the effect of outliers and metabolic shift due to spontaneous activity of the individual (Chabot et al. 2016b). Direct measures of AAS and FAS were then calculated according to Table 2 for all *S. acanthias* individuals with corresponding measures of MMR and SMR.

α was determined following the methods described in Seibel et al. (2021). First, instantaneous oxygen supply (α_0) was calculated for each respirometry measure period as $\alpha_0 = MO_2 / PO_2$, with PO_2 defined as the partial pressure of oxygen, recorded as the average PO_2 of each measure period. α was then defined as the highest α_0 value achieved during respirometry trials. To validate measured values of MMR, we additionally used Eq. (2) to calculate an alternative α, independent of measured MMR, where $MO_2 = \text{SMR}$ and $P_c = P_{cSMR}$ determined from the breakpoint method of P_c estimation (see Text S1).

$$\alpha = MO_2 / P_c \qquad (2)$$

$$\text{MMR} = P_{cMAX} \times \alpha \qquad (3)$$

We then predicted MMR based on the independently derived α (Eq. 2: $\alpha = \text{SMR} / P_{cSMR}$; Seibel et al. 2021), with $P_{cMAX} = 21$ kPa (the highest prevailing oxygen within *S. acanthias* range), using Eq. (3), for comparison with measured MMR.

2.9. Data analysis and thermal modeling of metabolic traits

All data and statistical analysis were performed in R versions 3.4.4 and 3.6.3 (R Core Team 2017, 2020). Welch's *t*-tests and paired *t*-tests were used to compare mean differences between metabolic metrics; SMR and RMR, measured versus predicted MMR, observed α versus $\alpha = \text{SMR}/P_{cSMR}$, and mass between the sexes. A Bonferroni correction was applied to all statistical comparisons of metabolic metrics, as multiple *t*-tests were used to make comparisons between metrics at a total of 5 temperatures. Thus, an alpha level of 0.01 was used as a more conservative threshold for determining statistical significance in order to control for the incidence of Type 1 error characteristic of multiple testing. In the case of mass comparison between the sexes (independent of temperature), no Bonferroni correction was required and an alpha level of 0.05 was used.

Permutational multifactor analysis of covariance (PermANCOVA) was used via 'aovperm' in the R package 'permuco' (Frossard & Renaud 2021) to assess the effect of temperature on the variation in each metabolic performance metric, with mass as a potential covariate. In addition, the effect of random error due to metabolic variation between individual sharks and the use of some individuals at more than one temperature was also assessed (see Text S1).

Mass was found to be a significant source of variation in *S. acanthias* metabolic data; thus, mass-specific metabolic traits (i.e. SMR, MMR, α, AAS, FAS) were normalized to a common body mass (population mean: 2.24 kg) using Eq. (4) to eliminate the effect of mass on metabolic trends.

$$MM = b_0 \times M^b \qquad (4)$$

where MM is the metabolic trait value, b_0 is a normalization constant, M is the mass of the animal, and b is a mass scaling coefficient for the metabolic trait values. Confident determination of a mass scaling coefficient for *S. acanthias* was not possible due to insufficient size range between adults in this study (<1 order of magnitude); thus, the common quarter-power scaling coefficient ($b = -0.25$; Kleiber 1932, Gillooly et al. 2001) was used. Quarter-power scaling was then used to correct individual performance metrics values to the study's average *S. acanthias* mass of 2.4 kg using the 'scale_MO2' function (R package respirometry v.1.3.0; Birk 2021) that additionally determined b_0 from the population sample within each temperature.

Thermal performance curves were then generated for all metabolic metrics to identify thermal 'optimality' or deficits in metabolic performance and aerobic scope. RMRs increase exponentially with temperature in most ectothermic species (Ege & Krogh 1914, Clarke & Johnston 1999, Clarke &

Fraser 2004). Therefore, SMR was modeled using an exponential curve. The 95% confidence bands were generated by bootstrapping via the 'bootMer' function (n = 5000 iterations) from the 'lme4' package (Bates et al. 2015).

MMR also typically increases exponentially but often plateaus or declines at higher temperatures. Due to high species variation in the relationship between MMR and temperature (e.g. see meta-analysis by Lefevre 2016), this metric has been modeled differently across previous studies and species. As such, Cullen and Frey graphs were implemented with bootstrap sampling (n = 1000 iterations) to determine the closest approximations of error distribution for MMR and α in this study. Using the 'fitdistrplus' package (Delignette-Muller & Dutang 2015), the 4 distributions in closet agreement with metabolic data were then compared via visual inspection of quantile–quantile, histogram and theoretical density, cumulative distribution frequency, probability–probability (PP) plots, and maximum likelihood. Logistic distribution yielded the best fit according to Akaike's information criterion (lowest AIC score) and was ultimately selected to represent the relationship between maximum performance metrics (MMR and α) and temperature within the experimental range. The logistic function was defined by a 3-parameter logistic equation:

$$y = \frac{A}{1 + \exp^{\frac{(B-x)}{C}}} \qquad (5)$$

where y represents the metabolic metric (MMR or α), x represents temperature, A represents the theoretical upper horizontal asymptote of the thermal curve, B is the temperature value at the inflection point of the logistic curve, and C represents a scaling parameter indicating the steepness of the increase in metabolic rate with temperature. The self-starting function 'SSlogis' ('stats' package v.3.6.3; R Core Team 2020) was used to determine each parameter of the thermal performance curve. Thermal performance curves for MMR and α were then fit using non-linear (weighted) least squares regression via the 'minpack.lm' package (Elzhov et al. 2016). Confidence bands were produced through bootstrap sampling (n = 5000 iterations) using the 'nlstools' package (Baty et al. 2015). Variance and 95% confidence intervals (2.5 and 97.5% quantiles) were calculated from the bootstrapped model predictions at each temperature.

A thermal performance curve for AAS was generated by subtracting modeled SMR from modeled MMR at each temperature (AAS = MMR − SMR). As AAS is a simple difference of random normally distributed variables, the variance of AAS at each temperature was calculated as the difference of the variance (σ) observed in the SMR and the MMR model predictions at each temperature. The 95% confidence intervals (CI) were thus calculated using Eq. (6), where the subscript t denotes the experimental temperature for AAS, SMR, and MMR at each given temperature.

$$\mathrm{CI} = \mathrm{AAS}_t \pm 1.96\sqrt{\sigma^2_{\mathrm{SMR}_t} + \sigma^2_{\mathrm{MMR}_t}} \qquad (6)$$

FAS was calculated as the ratio of the modeled MMR to the modeled SMR at each temperature (FAS = MMR / SMR). However, the expected variance of the ratio of random variables is difficult to compute and does not follow a normal distribution. Thus, we used a Monte Carlo simulation to estimate the 95% CI of the FAS at each temperature. At each temperature, we calculated FAS as the ratio of randomly simulated MMR and SMR values based on each variable's predicted mean and variance. This process was repeated 10 000 times, and the 2.5 and 97.5% quantiles of the simulated FAS were used to estimate confidence bands for FAS at each temperature.

Two distinct methods were then used to quantify the temperature sensitivity of each metabolic metric (SMR, MMR, α, AAS, FAS). The Q_{10} is a measure of the factorial change in metabolic metric for a 10°C change in temperature. A Q_{10} was calculated between means of metabolic metrics at 10 and 23°C in accordance with Eq. (7) for measured data binned by target temperature as well as for modeled means.

$$Q_{10} = \left(\frac{R_2}{R_1}\right)^{\left(\frac{10}{T_2 - T_1}\right)} \qquad (7)$$

Here, R_1 is the measured variable at a given lower temperature (T_1) and R_2 is that variable measured at a given higher temperature (T_2). E is the activation energy of metabolism, which represents the energy in electron volts (eV) that is required to activate the rate-limiting biochemical reactions that underly metabolic traits (Gillooly et al. 2001). E determines the rate of response (i.e. thermal sensitivity) of a metabolic trait within a given temperature range (Pawar et al. 2016). As metabolic reaction rates vary with temperature according to Boltzmann-Arrhenius relationships, in this study, E values were derived from Boltzmann-Arrhenius plots for all metabolic metrics. In these plots, the natural logarithm of each mass-corrected metabolic metric was plotted against inverse temperature, $1/k_\mathrm{B}T$, where k_B is Boltzmann's constant (relating thermodynamics and relative kinetic energy of gas particles) and T is the absolute temperature of the trial (K). In Arrhenius plots, E values were defined by the slope of the linear regression for each metric.

3. RESULTS

Of the 90 sharks captured, 71 successfully completed trials and were used in analyses (22 males, 49 females; 1.2–4.38 kg, mean: 2.24 kg; stretch total length: 71–94.5 cm; Table 1). Of the total 120 exercise trials conducted across temperature, 16 trials were unusable, 13 of which were excluded due to female sharks birthing in the chamber during measurement and the other 3 due to pump malfunctions. Of the total 40 hypoxia trials conducted across temperatures, 5 trials were unusable due to early removal of individuals that exhibited stress and a decline in condition regardless of PO_2. Mass-corrected metabolic results are reported below as means ± SD.

3.1. Metabolic traits

Metabolic rate at rest was 53.6–66.8% higher during exercise trials (RMR) than during hypoxia trials (SMR) at all temperatures (Fig. S3). Significant differences in RMRs between trial types (Welch's *t*-tests, $p < 0.01$; Table S1) suggest that the resting demands of *Squalus acanthias* continually decreased with time in the chamber (Chabot et al. 2016b) and support the use of resting rates derived from hypoxia trials (after the animals had been resting in the chamber for >22 h) to define SMR in this study (which by definition should describe the lowest metabolic rates measured in a conscious organism at rest). SMR increased exponentially with temperature between 10 and 23°C (Table 3, Fig. 2A), with a temperature sensitivity of $E = 0.59$ eV (Fig. 3) and $Q_{10} = 2.40$ across the measured range. Temperature had significant effects on SMR and MMR (PERMANCOVA; Table 4), as MMR was significantly increased with temperature (PERMANCOVA; Table 4) with a sensitivity of $E = 0.34$ eV and $Q_{10} = 1.65$ between 10 and 23°C (Table 3; Fig. 3). MMR did not decline at high temperatures. Modeled maximum performance produced a theoretical vertical asymptote at a temperature in excess of 30°C (Eq. 5; $A = 244.74$, $B = 10.11$, $C = 4.74$), with a lack of decline in maximum performance at the highest temperatures (Fig. 2A). However, it is important to point out that MMR may deviate from modeled curves beyond our measured thermal range (e.g. demonstrate rapid decay at critical temperatures). During MMR trials, the PO_2 declined from near air-saturation (21 kPa) to as low as 17.6 ± 1.41 kPa. However, MMR measured at trial PO_2 was not significantly different from that predicted at full air saturation (Eq. 3; Welch's *t*-tests, $p > 0.01$; Table S1). In general, *S. acanthias* reached exhaustion faster with shorter chase times as temperatures increased (chase time: $E = 0.73$ eV), likely as a result of faster muscle contraction and greater muscle power at higher temperatures (Bernal et al. 2005).

Values of α (mg O_2 kg^{-1} h^{-1} kPa^{-1}) significantly increased with temperature (PERMANCOVA; Table 4) between 10 and 23°C, with a temperature sensitivity ($E = 0.39$ eV, $Q_{10} = 1.74$) similar to that for MMR. There was no decline in α at the highest measured

Table 3. Mean metabolic traits and temperature sensitivities binned by target temperature for *Squalus acanthias*. Measures are mass-corrected to the population mean (2.24 kg) and reported as means ± SD. Q_{10} values are represented as a ratio, calculated between 10° and 23°C for all metrics, and E values are represented in electron volts (eV). MMR: maximum metabolic rate; SMR: standard metabolic rate (hypoxia trials); RMR: resting metabolic rate (exercise trials); α: oxygen supply capacity; AAS: absolute aerobic scope; FAS: factorial aerobic scope. NA: not applicable

	SMR (mg O_2 kg^{-1} h^{-1})	MMR (mg O_2 kg^{-1} h^{-1})	α (mg O_2 kg^{-1} h^{-1} kPa^{-1})	AAS (mg O_2 kg^{-1} h^{-1})	FAS (ratio)	Chase time (s)
10°C[a]	27.94 ± 7.22	120.98 ± 27.65	6.52 ± 1.67	84.2 ± 18.7	4 ± 0.96	457.42 ± 169.43
13°C[a]	39.46 ± 11.73	175.96 ± 35.33	9.62 ± 2.61	147.79 ± 29.85	4.76 ± 1.9	498.65 ± 156.46
17°C[a]	55.79 ± 12.64	190.49 ± 36.32	10.38 ± 2.4	153.71 ± 29.55	3.95 ± 1.51	343.1 ± 123.08
21°C[a]	72.37 ± 10.33	230.32 ± 49.88	13.21 ± 3.5	223.42 ± 50.6	3.83 ± 0.78	377.30 ± 126.46
23°C[a]	73.23 ± 6.48	226.91 ± 49.96	13.33 ± 3.31	166.75 ± 30.29	3.17 ± 0.45	301.95 ± 92.27
Q_{10}[a]	2.10	1.62	1.73	1.69	0.84	0.73
Q_{10}[b]	2.40	1.65	1.74	1.39	0.69	NA
E[b]	0.59	0.34	0.39	0.25	-0.25	0.73

[a] Calculated from target temperature binned means

[b] Calculated from modeled means (Fig. 2) at each target temperature

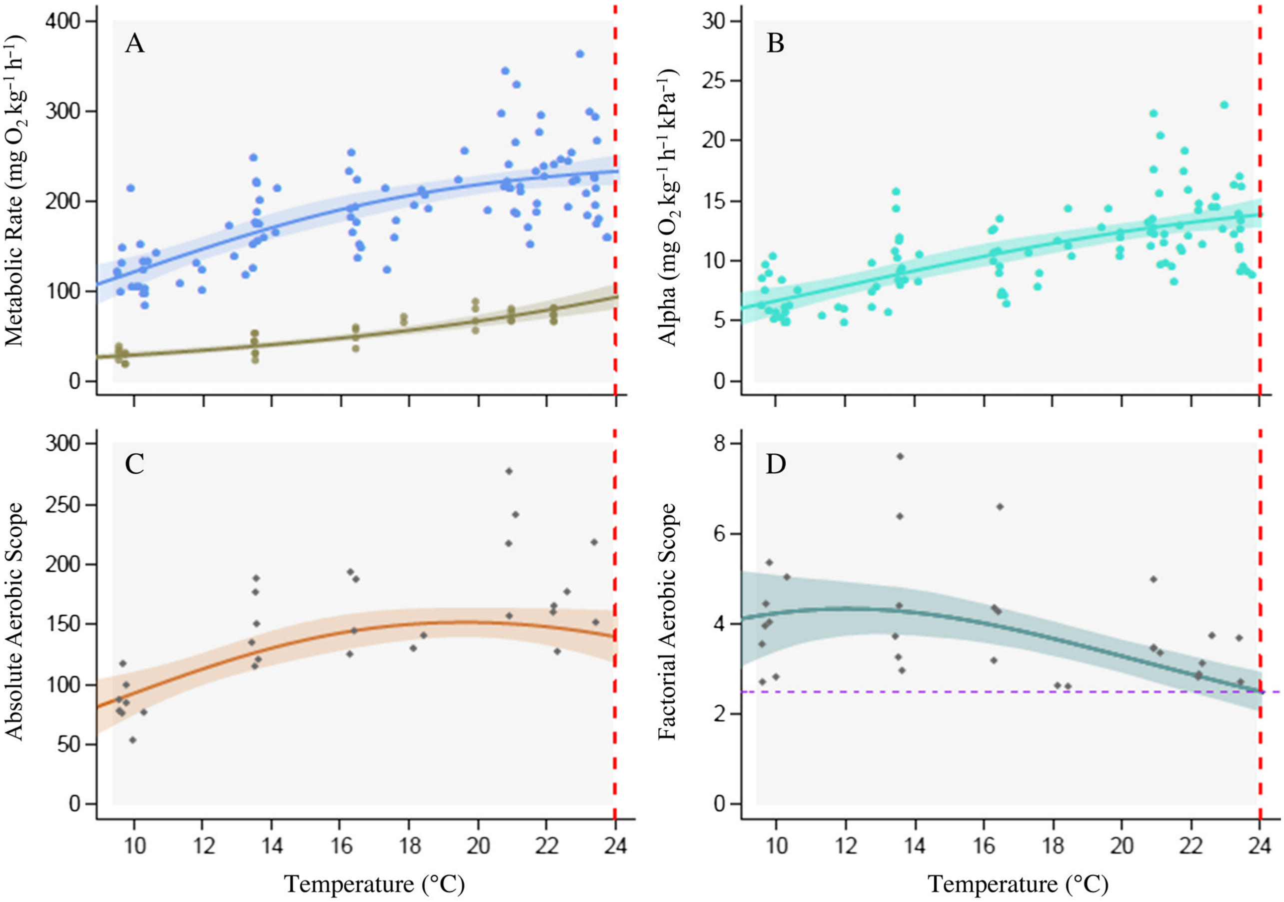

Fig. 2. Thermal performance curves for *Squalus acanthias* showing (A) maximum metabolic rate (MMR; royal blue) and standard metabolic rate, (SMR; olive), (B) oxygen supply capacity (α), (C) modeled absolute aerobic scope (AAS) derived from subtracting modeled SMR from modeled MMR, and (D) modeled factorial aerobic scope (FAS) derived from the quotient of modeled MMR to modeled SMR. Solid lines model thermal performance of each metabolic metric; solid circles in (A) and (B) represent directly observed individual metabolic measurements. Shaded regions: 95% CIs for each model; vertical red dashed lines: potential critical upper thermal limit for *S. acanthias* found in this study; gray shaded regions: thermal region within which data was collected. The horizontal purple dashed line in (D) represents a theoretical population limiting threshold at FAS = 2.51. Filled black diamonds in (C) and (D) represent measures of AAS and FAS from individuals that completed both exercise and hypoxia trials, separate from modeled AAS and FAS (see Sections 2.8 & 2.9)

temperatures. Modeled α also produced a theoretical peak in excess of 30°C (Eq. 5; $A = 244.74$, $B = 10.11$, $C = 4.74$), with no decrease in oxygen supply within the measured thermal range. The observed α was not significantly different than α calculated from P_{cSMR} determined using the breakpoint method, with the exception of 23°C (Welch's *t*-test, $t_{24.935} = 4.0288$, $p = 0.00046$; Table S1). Thus, throughout the natural temperature range, α was similar whether determined at rest in hypoxia or during maximum exertion in air-saturated waters. This suggests that MMR declines linearly with oxygen from P_{cMAX} to P_{cSMR} (Figs. 4 & 5).

AAS increased significantly with temperature (PERMANCOVA; Table 4). Direct measures of AAS ($E = 0.41$ eV) peaked at 21°C, with a decline between 21 and 23°C that could not be statistically evaluated due to low sample size at the 21°C temperature bin ($n = 4$). By contrast, modeled AAS (Fig. 2C), which encompassed the entire population of MMR measurements rather than only those animals that completed both exercise and hypoxia trials, increased with a slightly lower temperature coefficient ($E = 0.25$ eV), and produced a more reliable estimate of AAS. Modeled AAS peaked at ~19.5°C with a non-significant decline between the peak and 23°C as indicated by strongly overlapping CIs (Fig. 2C).

FAS scaled inversely with temperature, with a temperature sensitivity of $E = -0.12$ eV for direct measures and $E = -0.25$ eV for modeled values ($Q_{10} = 0.74$). Modeled FAS reached a minimum ratio of ~2.7 at 23°C and was a more reliable estimate of FAS (Fig. 2D).

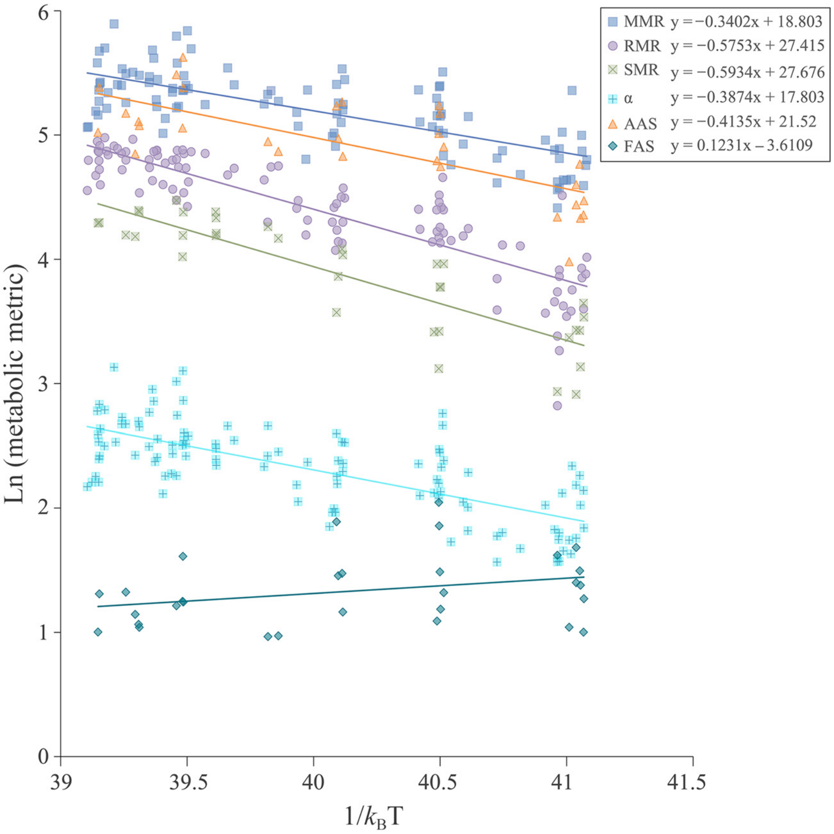

Fig. 3. Arrhenius relationships of metabolic metrics for *Squalus acanthias* trials. Temperature sensitivities, *E* (eV), are derived from each slope, where k_B is Boltzmann's constant and *T* is temperature (K). Negative slope indicates an increase with temperature (°C). MMR: maximum metabolic rate; RMR: resting metabolic rate (exercise trials); SMR: standard metabolic rate (hypoxia trials); α: oxygen supply capacity; AAS: absolute aerobic scope; FAS: factorial aerobic scope

3.2. Sex differences and the effect of mass

Experimental groups for *S. acanthias* across temperatures ranged from 19 to 47% male (Table 1). There was a significant difference in mass between the sexes (Welch's *t*-test, $t_{101.31} = 14.33$, $p = 2.2 \times 10^{-16}$), with females on average 1.07 kg larger (1.73× the mass of males) and 10.05 cm longer than their male counterparts (Table 1). Though mass was not found to be a covariate of temperature, mass did significantly affect the variance in SMR, MMR, and α across temperatures (PERMANCOVA; Table 4) for mass-specific values. Larger female sharks generally had lower mass-specific metabolic rates than smaller male sharks (Fig. S4). However, after normalizing to a common mass (using Eq. 4), there was no significant effect of sex on MMR or α (Table S1). The smaller sample size for hypoxia trials (Table 1) precluded reliable statistical comparisons between sexes for SMR, P_{cSMR}, and direct measures of aerobic scope.

3.3. Loss of equilibrium and mortality

All sharks at rest (and periodically during swimming in holding) exhibited a loss of equilibrium at ⩾20°C regardless of ambient PO_2 (Fig. 6). Equilibrium loss was remedied when sharks were returned to 18°C with no

Table 4. Permutational ANCOVA results of metabolic metrics by target temperature bin for *Squalus acanthias* trials. MMR: maximum metabolic rate; SMR: standard metabolic rate (hypoxia trials); RMR: resting metabolic rate (exercise trials); α: oxygen supply capacity; AAS: absolute aerobic scope; FAS: factorial aerobic scope; p(perm)-values were calculated from permutational ANCOVA; **bold** values are significant ($p \leqslant 0.05$)

Variable	Effect	df	Pseudo *F*-value	Resampled p (perm)-value
MMR	Temperature	4	29.145	**0.0002**
	Mass	1	55.134	**0.0002**
	Mass × temperature	4	2.136	0.0834
SMR	Temperature	4	33.4453	**0.0002**
	Mass	1	13.6023	**0.0012**
	Mass × temperature	4	0.7361	0.5740
RMR	Temperature	4	85.8228	**0.0002**
	Mass	1	29.1065	**0.0002**
	Mass × temperature	4	0.5853	0.6700
α	Temperature	4	23.7358	**0.0002**
	Mass	1	41.2323	**0.0002**
	Mass × temperature	4	0.8728	0.4634
AAS	Temperature	4	2.477×10^{-5}	**0.0002**
	Mass	1	0.00719	0.9310
	Mass × temperature	4	1.12853	0.3740
FAS	Temperature	4	1.8866	0.1524
	Mass	1	1.2143	0.2786
	Mass × temperature	4	0.5707	0.6930

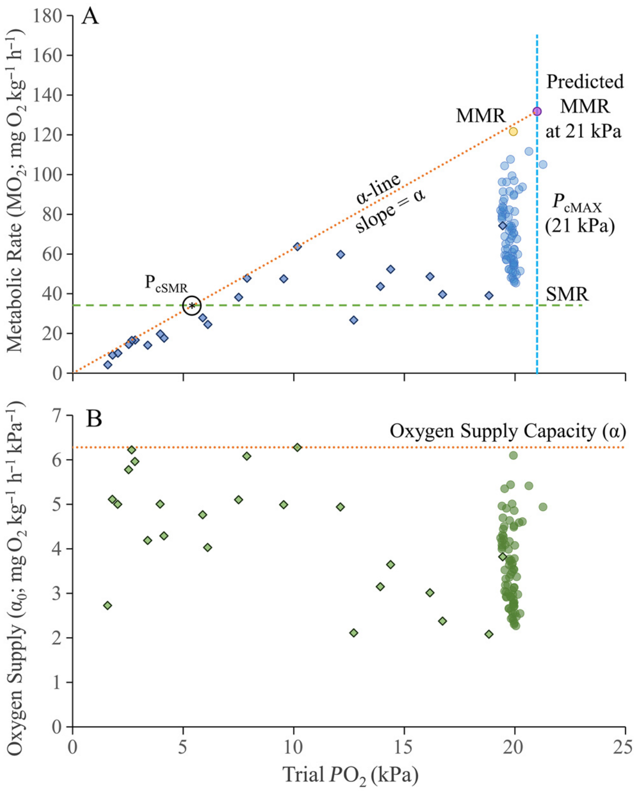

Fig. 4. Metabolic rates, the alpha line, and oxygen supply for a representative *Squalus acanthias*. (A) Oxygen consumption rates (MO_2; filled blue circles are from exercise trials; filled blue diamonds are from hypoxia trials) for each closed measure period of exercise and hypoxia trials. The α-line ($MMR = \alpha \times PO_2$) describes the oxygen dependency of maximum metabolic rate (MMR) between P_{cMAX} and P_{cSMR}. P_{cSMR} is the partial pressure of oxygen (PO_2) at which standard metabolic rate (SMR) intersects the α-line. P_{cMAX} (dashed teal line) is the PO_2 at which MMR becomes oxygen-dependent, assumed to be 21 kPa for this species. MMR (yellow circle) and predicted MMR at 21 kPa (purple circle) are shown at the trial PO_2 and P_{cMAX}, respectively. (B) Oxygen supply (filled green circles are from exercise trials; filled green diamonds are from hypoxia trials) for closed measures pictured in (A) represent the oxygen physiologically supplied per unit available pressure ($\alpha_0 = MO_2/PO_2$). Oxygen supply capacity (dotted line) is the maximum oxygen supply demonstrated for the same individual

overt residual issues. Interestingly, swimming at high temperatures during chase protocols appeared unaffected. Attempts to acclimate sharks for further testing at 25°C resulted in 41.6% mortality (n = 5 of 12 individuals in the experimental group) within the first 36 h of exposure to water ⩾24°C, with 33.33% of that mortality occurring within 12–24 h

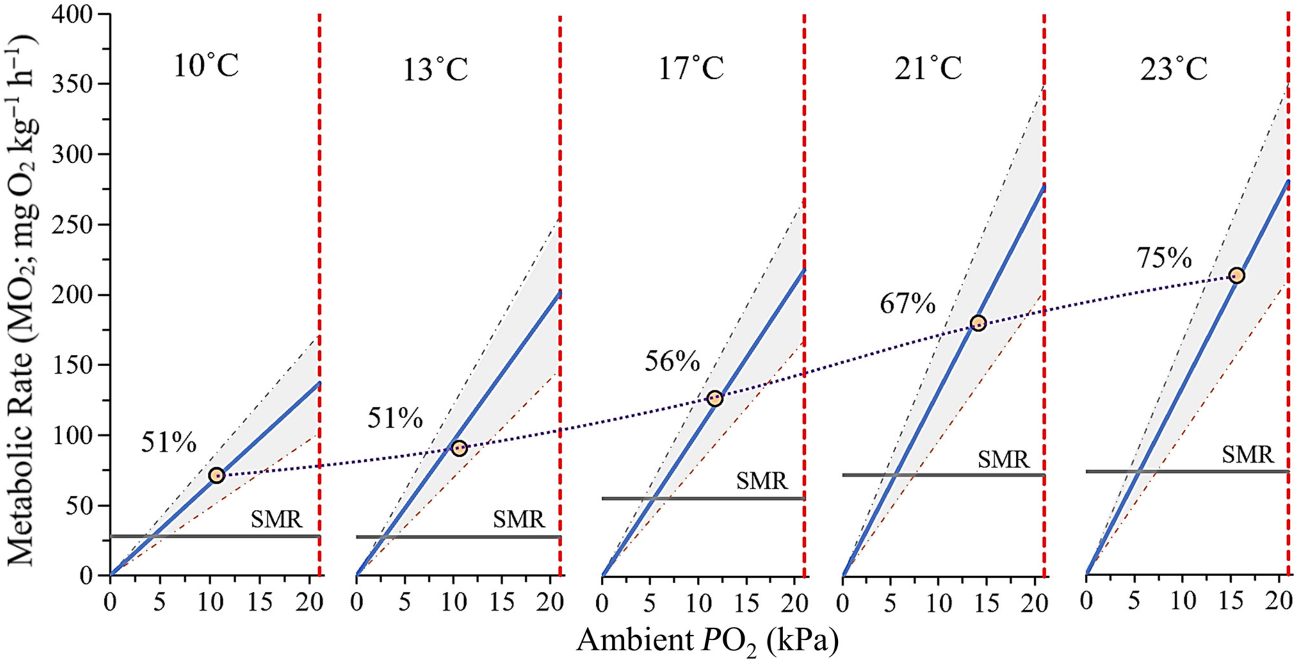

Fig. 5. Average oxygen and temperature dependency of maximum metabolic rate (MMR) for *Squalus acanthias*. Blue solid line passing through the origin: average α-line ($MMR = \alpha \times PO_2$; describes the oxygen dependency of MMR) at each temperature bin extrapolated to a P_{cMAX} (the PO_2 at which MMR becomes oxygen-dependent) of 21 kPa (air-saturation, red dashed lines); gray shaded section: standard deviation of the α-line at each temperature. Orange-filled circles: average MMR and oxygen level at which a factorial aerobic scope (FAS) of 2.5 (demonstrative critical FAS) would occur at each temperature based on our modeled averages. Percentages: % air saturation (% of 21 kPa) at which the FAS of 2.5 occurs; purple dashed line: how an FAS of 2.5 changes across temperature and O_2

Fig. 6. *Squalus acanthias* individuals displaying loss of equilibrium at rest (⩾20°C). Oxygen in holding tanks substantially exceeded P_{cSMR} (the oxygen level that limits the ability to support standard metabolic rate), indicating that oxygen limitation is not the cause of the loss of equilibrium. Righting reflex was restored when sharks were returned to cooler temperatures (18°C)

of exposure. Abnormal or sporadic swimming or loss of equilibrium have previously been used as identifiers of physiological stress and critical thermal limits for fish species (e.g. Elliott & Elliott 2010, Brauner & Richards 2020). The observation of mortality during acclimation to high temperatures (⩾24°C) was similar to studies identifying incremental thermal maximum (critical upper temperature resulting in death after low rates of temperature increase e.g. 0.25°C d^{-1}; Lutterschmidt & Hutchison 1997, Zanuzzo et al. 2019, Bartlett et al. 2022) and the incremental thermal maximum-like stress resulting in morbidity in aquaculture scenarios (Brauner & Richards 2020). These abnormal behaviors were noted during routine observation of *S. acanthias* in holding and during limited opportunistic observation in trials. Such behavioral observations served to identify conditions that induced overt stress in *S. acanthias*, identify potential suboptimal temperatures, and try to estimate critical limiting temperatures within the thermal range during experimentation or acclimation.

4. DISCUSSION

This study evaluated thermal sensitivity of several metabolic traits for *Squalus acanthias* of the US NES. Oxygen supply and aerobic scope were evaluated for their contribution to thermal tolerance limits, as was the ability of aerobic scope to inform thermal optimality and sublethal thermal limits for *S. acanthias*. Here, we present the first measures of energetic demands from rest to maximum performance, α, and aerobic scope for this species in the Atlantic. We further discuss the implications of our findings in predicting viable habitat for *S. acanthias*, the universality of aerobic scope as a predictive limiting metric across species diversity, and other considerations for thermal tolerance and biogeographic responses of *S. acanthias* in an era of climate change. As average temperatures within the US NES continue to rise outside of the species' occupied thermal envelope and the frequency of acute heating events increases, sublethal and critical upper thermal limits become a key constraint on viable habitat.

4.1. Thermal sensitivity

The temperature sensitivity of SMR was in the range for most coastal marine species (E mean: ca. 0.6–0.65 eV; Huey & Kingsolver 2011, Deutsch et al. 2020), while that of MMR (E = 0.34 eV) was considerably lower, resulting in declining FAS as temperature increases. Diminished aerobic scope at high temperatures is widely believed to determine thermal tolerance limits and, thus, biogeography. Moreover, oxygen limitation at high temperatures is also proposed to limit aerobic scope (e.g. Pörtner & Knust 2007, Farrell et al. 2008, Pörtner 2010, Eliason et al. 2011) by a failure of the cardiorespiratory system to increase oxygen supply to tissues at a rate that supports the rise in basic demands at higher temperatures (Clarke & Johnston 1999, Lefevre 2016). However, failure of oxygen supply and aerobic scope do not universally explain species' thermal limits (e.g. Ern et al. 2016, Lefevre 2016, Jutfelt et al. 2018, Seibel & Deutsch 2020). Outside the evolved thermal range, any number of processes including α may fail (e.g. protein unfolding, cytoskeleton network collapse, errant localization of organelles, reduced mitochondrial function, morphological changes in membranes, aberrant RNA splicing: Richter et al. 2010; loss of neurological function: Prosser & Nelson 1981, Prosser 1991, Ern et al. 2015, etc.) as there is reduced selective pressure to preserve function at temperatures outside the natural range. Reduced aerobic scope at high temperatures may also result from a failure of the metabolic machinery to use oxygen (e.g. muscle oxidative performance) or an inability of the muscles to produce equivalent work rather than an inability to provide sufficient oxygen (e.g. Slesinger et al. 2019). In addition, animals may be limited by temperatures that constrain processes vital for fitness, such as growth or reproduction, long before temperatures are reached that may limit aerobic scope or oxygen supply (Clark et al. 2013).

In the present study, we found no evidence that oxygen supply limits active metabolism at the tested levels or that aerobic scope constrains thermal tolerance in *S. acanthias* under normoxic conditions. In this study, maximum performance and AAS were not diminished at thermal limits. Additionally, α increased in direct proportion to MMR, supporting the findings of Seibel & Deutsch (2020) that α has evolved to support MMRs at the prevailing oxygen pressure. Parallel trends in MMR and α suggest that as temperatures increase, physiological adjustments (e.g. Gräns et al. 2014) are made at various steps along the oxygen supply chain to accommodate elevated demands in *S. acanthias* (Seibel & Deutsch 2020), with such adjustments occurring even as estimated critical temperatures were approached. For example, oxygen supply adjustments may include increased cardiac output as a result of increases in heart rate or stroke volume (Farrell 2002, Clark et al. 2008), increased ventilation (Burton 1979), increased blood oxygen carrying capacity via increased red blood cell volume (Muñoz et al. 2018), or changes in oxygen exchange surfaces within the body to promote increased extraction or diffusion rates (Sollid & Nilsson 2006).

For this population of dogfish, 24°C was estimated to be a critical temperature (although true designation would require separate traditionally defined critical thermal maximum (CT_{MAX}) trials). Overall, there appears to be selection for maximum performance, oxygen supply, and adequate aerobic scope to be maintained at high temperatures, up until the point of estimated critical thermal limits for *S. acanthias*. Thus, a sublethal upper limiting temperature cannot be indicated by a significant decline in AAS or α for this species.

AAS increases continuously up to ~19.5°C, whereafter it plateaus to 23°C. The temperature range across which AAS peaks cannot be considered an optimal temperature range for this species as these temperatures resulted in a loss of equilibrium regardless of environmental PO_2. Loss of equilibrium typically indicates physiological stress and a loss of neuromuscular function, which is commonly used to identify behavioral impairment (Davis 2010, Raby et al. 2012, Holder et al. 2020, Whitney et al. 2021), hypoxic thresholds (Speers-Roesch et al. 2013, Borowiec et al. 2016, Wood 2018, Borowiec et al. 2020), acute upper thermal tolerance (Beitinger & Lutterschmidt 2011), and CT_{MAX} (Elliott & Elliott 2010, Brauner & Richards 2020). In this study, loss of equilibrium occurred at oxygen saturation well above determined P_{cSMR} and without a detriment to aerobic scope or maximum capacity. Equilibrium was restored when the temperature was lowered to 18°C, suggesting that its loss was a result of thermal stress and not oxygen limitation.

Reported habitat use for wild *S. acanthias* also suggests that such high temperatures are not preferred by *S. acanthias*. Catch frequency for this species is generally highest between 6 and 15°C (Jensen 1966, Castro 1983, McMillan & Morse 1999, Stehlik 2007, Bockus et al. 2020; although many of these studies have also reported less frequent landings at temperatures as low as 4°C, up to 22°C), and despite a large thermal range occupied by *S. acanthias*, preferred *in situ* temperatures for satellite-tagged individuals (inclusive of the study region) were skewed to colder values (9–13°C; 2–3 yr satellite tags; Carlson et al. 2014). Additionally, Bockus et al. (2020) identified thermal stress at 21°C via a 3-fold elevation in heat-shock proteins (vital in the protection of protein structure and function against thermal stress; Richter et al. 2010) relative to 15°C controls for *S. acanthias*. Such mounting physiological evidence of the onset of thermal stress around temperatures in which AAS peaks, and ecological evidence of preference for cooler temperatures, make it difficult to reconcile peak AAS with thermal optimality for *S. acanthias*.

Although AAS was highest at the warmest temperatures, SMR was elevated by >2.5 times. Greater effort is then required for foraging activities to support elevated caloric demands at high temperatures. These additional energetic costs must be weighed against potential advantages (if any) in growth rate, scope for predator evasion, or reproductive output at higher temperatures (discussed below). Moreover, the effect of temperature on the costs of growth or reproduction for this species is unknown. More active, ram ventilating, highly migratory, pelagic species such as mahi-mahi *Coryphaena hippurus* benefit from most often residing in the tight thermal range (24–29°C; Hammond 2008, Farrell et al. 2014, Merten et al. 2014b) that provides their greatest aerobic capacity and swim speed performance (Heuer et al. 2021). Mahi-mahi swim continuously and have higher relative metabolic demands (Heuer et al. 2021) than *S. acanthias*, are significantly more fecund, and have one of the highest known growth rates for teleost species (Palko et al. 1982, Benetti et al. 1995, Merten et al. 2014a,b). For the less active, benthopelagic *S. acanthias*, which has low growth rates and low fecundity and does not need to swim continuously to breathe, it appears as though maximized aerobic scope is not worth the trade-off of residing at higher temperatures that require continuously elevated metabolic demands. These findings are in contrast to the oxygen- and capacity-limited thermal tolerance (OCLTT) hypothesis that promotes oxygen limitation and constrained aerobic scope as the universal primary drivers of upper thermal tolerance (Pörtner 2010).

4.2. FAS and viable habitat

Other prevailing metabolic theories such as the metabolic index (Deutsch et al. 2015, Deutsch et al. 2020) focus instead on delineating viable species habitat based on the minimum FAS that is required to sustain individual survival as well as population success. A survey of diverse marine species previously demonstrated that the warm end of species' natural distribution is coincident with an FAS near 3. In other words, the environmental PO_2 must exceed a species' P_{cSMR} by about 3× (Deutsch et al. 2015, 2020). However, in *S. acanthias*, FAS reaches a minimum of 2.7 at 23°C, near the estimated critical temperature. Thus, FAS does not appear to be limiting (Table 3, Fig. 4), as thermal tolerance is already failing at 20°C due to factors other than oxygen or energy supply, such as reduced protein function (Bockus et al. 2020).

Our results suggest that if a particular value of FAS can limit dogfish populations, it may only be reached at lower environmental oxygen conditions. For example, limited data shows current DO levels in the US NES are thought to reach as low as ~80% air saturation across the shelf (Slesinger et al. 2024) (although there is poor spatiotemporal oxygen data resolution). Air saturation of 75% would reduce FAS to values below 2.7, even within the tolerated temperature range (Fig. 5). While the US NES does not have large-scale oxygen minimum zones like those characteristic of equatorial upwelling zones (e.g. western coasts of North and South America, Africa, and the Indian Ocean), hypoxic episodes have been recorded in estuaries and coastal waters of the US North Atlantic (6–35% of surveyed sites) and Mid-Atlantic regions (42–64% of surveyed sites) since the 1980s into the 2000s (Jewett et al. 2010), as symptoms of anthropogenic coastal nutrient loading. Therefore, although aerobic scope does not primarily limit thermal tolerance in this species in normoxia (air saturation), as oxygen saturation declines with rising ocean temperature and depth, and instances of hypoxia are becoming more prevalent in coastal waters globally (Diaz & Rosenberg 2008, Diaz & Breitburg 2009, Zhang et al. 2010), oxygen limitation of aerobic scope could contribute to habitat shifts for *S. acanthias*. However, to determine a true critical FAS for this species and whether it is likely to be limiting under future environmental scenarios, more fine-scale ecological data on *S. acanthias* movement, abundance, and distribution in relation to temperature and oxygen is needed, along with better oxygen and temperature data resolution at depth on the US NES. It is clear further investigation is required to identify the nuances of the effects of interacting abiotic variables on thermal tolerance and viable habitat.

4.3. Other considerations for thermal tolerance and biogeographic responses under climate change

Ultimately, the ability of ectothermic species to survive and thrive as climate change intensifies (Scheffers et al. 2016, Pecl et al. 2017, IPCC 2019) will depend on myriad factors. Current physiological capabilities, capacity for acclimation and/or adaptation to new conditions, the rate of environmental change (Nguyen et al. 2011, Pinsky et al. 2013), and ecological factors such as how heavily species rely on certain prey items, may influence species biogeographical responses to climate change.

While *S. acanthias* have been observed to vertically migrate in pursuit of abundant prey resources such as longfin squid (Stehlik 2007, Sagarese et al. 2014), and trends in the distribution of various size classes have been correlated with general prey abundance (Sagarese et al. 2014), *S. acanthias* are considered generalist predators. They demonstrate opportunistic feeding with a diet that reflects local prey abundance (Moustahfid et al. 2010) and is subject to changes in time, environmental factors (specifically temperature), and geographic location (Stehlik 2007, Dell'Apa et al. 2015). These animals have also been highly successful in filling vacated trophic niches (Link & Garrison 2002) and dominate as piscivores in their ecosystems. In addition, previous research has identified potentially increased top-down influence of *S. acanthias* across the US NES under current warming scenarios, with a potential 2-fold increase in overlapping habitat for prey *S. acanthias* has less interaction with at low temperatures (Selden et al. 2018). Bearing that in mind, distributional responses of *S. acanthias* under elevated temperature scenarios are unlikely to be governed by the thermal tolerances of specific prey items, but rather by their own abilities to tolerate, acclimate, and/or adapt to environmental change on various time scales.

As ocean warming continues, exposure to stressful temperatures within the currently occupied range of this species is expected to rise. However, there exists limited information on the proportion of time that *S. acanthias* currently spend near their thermal limits or with what regularity these sharks move through potentially challenging thermal environments. This study quantified metabolic responses of *S. acanthias* that were incrementally acclimated to target temperatures over the course of days. Changes in this timeframe reflect the abilities of *S. acanthias* to cope with acute changes in temperature and 'stints' at elevated temperatures, particularly relevant in the face of increased daily thermal fluctuations and increasing intensity and frequency marine heatwaves (Easterling et al. 2000, Meehl & Tebaldi 2004, Rahmstorf & Coumou 2011, Stocker et al. 2013, Oliver et al. 2018). Heat anomalies +2−7°C occur across the US NES with the greatest frequency in the Mid-Atlantic Bight (Schlegel et al. 2021, Großelindemann et al. 2022) and can last between 5 and 400 d (Oliver et al. 2018). Thermal sensitivity and the capacity for thermal acclimation on longer time scales (weeks, months, etc.) may be equally important for predicting organism responses and limiting thermal thresholds under extended heatwaves and long-term warming trends characteristic of climate change. Acclimation can increase thermal tolerance by reducing metabolism relative to the initial acute thermal change, modulating SMR and aerobic scope, and allowing for compensation of direct thermodynamic effects on metabolism (Precht 1958, Johnston & Dunn 1987, Angiletta 2009, Schulte et al. 2011, Seebacher & Franklin 2012, Sandblom et al. 2014, Bouyoucos et al. 2022, Johansen et al. 2021, Wheeler et al. 2022). The acute thermal stress we observed coincided with results from studies that had longer acclimation times, and with thermal limits revealed by satellite-tagged individuals within the study region. However, long-term thermal acclimation requires further investigation to quantify the limits of physiological plasticity in thermal tolerance for *S. acanthias*. Additionally, although thermal adaptation to high temperatures is possible, for many marine species, climate change is occurring faster than the rate of adaptation through natural selection (Gienapp et al. 2008, Reusch 2014, Fox et al. 2019). *S. acanthias* are long-lived, late to mature (females ~12 yr, males ~6 yr; Nammack et al. 1985, Burgess 2002, Castro & Peebles 2011), with low fecundity (1−15 pups per reproductive cycle in the NW Atlantic; Colvocoresses & Musick 1980, Burgess 2002) and long gestation (18−24 mo; NEFSC 2006). Thus, adaptation seems unlikely to keep pace with the rapid rate of environmental change on the US NES, given the slow generational turnover.

Responses to both acute and long-term warming outside of tolerance thresholds for this species could include poleward shifting distributions, more frequent use of offshore habitats, or a change in occupied depths that could ultimately lead to shifts in core habitat use or decreased residency times (Nye et al. 2009, Kleisner et al. 2017, Morley et al. 2018). While poleward distributional shifts have not been reported for *S. acanthias* to date, the extensive range of this species outside the bounds of study surveys (Nye et al. 2009) has made previous assessments of responses to climate change difficult to interpret. For both the northern and southern parts of the stock, the highest mean daily temperatures experienced by *S. acanthias* occurred in months when they used the shallowest habitat (<50 m; mean daily depth 50 m, summer; Carlson et al. 2014). Tagged *S. acanthias* have ranged from the surface to depths of 481.5 m (northern tags) and 214.5 m (southern tags), with individuals occupying a range of depths throughout the day. Maximum depths for *S. acanthias* have also been reported to reach 500−900 m (Compagno 1984, Stehlik 2007), suggesting that vertical displacement to deeper waters in pursuit of thermal refuge may also be a viable strategy in times of thermal stress. Marine heatwaves occur both at the surface and at depth. They are especially intense (up to +7°C anomaly) at depths between 100 and 150 m on the US NES (Großelindemann et al. 2022) and have been recorded as deep as 300 m globally (Ryan et al. 2021), depths that *S. acanthias* also regularly occupy. Such events may not necessarily limit aerobic performance, but they may compress the habitat available to optimize fitness-related traits. However, the percentage of currently occupied habitat that would need to warm beyond sublethal thermal limits to induce shifts in habitat association for this species is unknown, as is the rate and duration of thermal change that may induce biogeographical changes. It is also unknown whether trends in thermal performance and tolerance are the same across the species range or whether there are differences between *S. acanthias* groups or latitudinally distinct populations.

Results from this study demonstrate metabolic demands and associated α are related to size in *S. acanthias* (Table 4, Fig. S4). Smaller animals had a higher per kg tissue (mass-specific) metabolic rate than larger conspecifics, despite the greater overall (non-mass-specific) metabolic demand in larger animals (Fig. S4). *S. acanthias* schools by size prior to sexual maturity and by sex as well as size after maturity (Ford 1921, Shepherd et al. 2002, Stehlik 2007, Dell'Apa et al. 2014). Thus, schooling individuals of similar size should have similar metabolic demands, and this lends support to the idea that this species schools according to metabolic needs (see Dell'Apa et al. 2015). When the effect of mass was removed, *S. acanthias* did not demonstrate significant differences in metrics between the sexes; thus, metabolic differences between sexes in *S. acanthias* also appear largely related to size (Fig. S4), although we were unable to tease apart the specific effects of gestation and reproductive investment on metabolic metrics (see below). Between adults of this population, however, it appears that size alone (<1 order of magnitude difference) may not be enough to drive differential thermal tolerance between the sexes, given that mean temperature differences did not exceed 1°C between the sexes in satellite-tagged adult wild *S. acanthias* (Carlson et al. 2014, see also Shepherd et al. 2002). Although the effect of growth or reproduction on metabolic demands and temperature sensitivity in *S. acanthias* was outside the core objectives of this study, mass-related results may indicate that ontogenetic differences may impact thermal sensitivity of *S. acanthias* as in other species (Harris 1952, Moore 1998, Shepherd et al. 2002, Pistevos et al. 2015).

We were unable to tease apart the specific effects of gestation and reproductive investment on metabolic metrics. Given that mature *S. acanthias* females spend the majority of their time in gamete investment and gestation, the impact of reproduction requires further consideration in the responses of *S. acanthias* to rising temperatures. *S. acanthias* has one of the longest gestation periods of any vertebrate species at 18–24 mo (NEFSC 2006), exhibits simultaneous follicular maturation and gestation (Demirhan & Seyhan 2006) as well as the ability to simultaneously carry pregnancies of different gestational stages within one individual (observed in this study). As mating occurs immediately after parturition (Jensen 1966, Hanchet 1988), mature *S. acanthias* females are continuously investing in reproduction. Although we were not able to distinguish the effects of gestational stage in *S. acanthias*, oxygen demand increases during gamete production in many marine species (Masonjones 2001, Kraffe et al. 2008, Madeira et al. 2012). Additionally, for live-bearing species like *S. acanthias*, the increasing oxygen demands of developing embryos add to the metabolic burden and may impose further constraints on upper thermal tolerance in carrying females (Dygert & Gunderson 1991, Baeza & Fernández 2002, Timmerman & Chapman 2003, Green & McCormick 2005, Auer et al. 2021).

Females of several fish species enter warmer coastal waters to take advantage of temperatures that accelerate parturition (Moore 1998, Shepherd et al. 2002), embryo development (Harris 1952, Pistevos et al. 2015), gestation (Hight & Lowe 2007, Jirik & Lowe 2012, Nosal et al. 2014), and in the case of *S. acanthias*, warmer waters would also increase aerobic scope for other vital activities (e.g. foraging and locomotion to support elevated demands of pregnancy). However, warmer waters also elevate the cost of all demands, including associated costs of pregnancy, and there is very clearly a point of diminishing returns. Given that temperatures at which aerobic scope is maximized in this species coincide with stress and impaired neural function, reproductive investment and gestation are not optimized at peak aerobic scope (19.5°C), in contrast to the OCLTT theory. Furthermore, if pregnant females have higher metabolic demands, they may demonstrate heightened vulnerability to climate shifts and habitat loss than conspecifics, as the thermal window for reproduction is often much smaller than the thermal window for activity (Fry 1971, Dahlke et al. 2020b). Future temperature-controlled studies of metabolic demand throughout gamete investment and gestation are warranted for this species.

It is also key to consider variations in thermal sensitivity and tolerance between portions of a managed stock. Due to the propensity for long migrations and the wide species distribution, *S. acanthias* is managed as a single stock on the US Atlantic coast (ASMFC 2002). Genetic data support a single, randomly breeding population throughout the western North Atlantic (Hisaw & Albert 1947, Veríssimo et al. 2010, Veríssimo et al. 2011). However, there is mounting evidence of subgroups or subpopulations that exhibit distinct movement patterns, seasonal distributions, thermal associations, and more limited intermixing than previously assumed (Campana et al. 2008, 2009, Campana 2010, Rulifson 2010, Rulifson et al. 2012a, Carlson et al. 2014). *In situ* satellite data from *S. acanthias* (Carlson et al. 2014) revealed that the northern group (tagged in the Gulf of Maine) stayed primarily around the Gulf of Maine, with a portion of the population spending autumn and winter off the coast of New York and New Jersey. The southern group (tagged off Cape Hatteras) spent winter and spring south of Delaware, migrating north for summer into New Jersey, with autumn being the only season with spatial overlap in 50% utilization distributions between the northern group and southern group (New York and New Jersey). Northern groups and southern groups also significantly differed in mean overall temperature (~3.5°C higher in the southern group), mean seasonal temps (~2–5°C higher for the southern group), mean overall depth (nearly 3-fold deeper for the northern group, ~65.7 m deeper), mean seasonal depth (27.9–88.4 m deeper for the northern group in winter, spring, summer). In addition, individuals captured off Cape Hatteras, NC, appear to spend more time at elevated temperatures (⩾21°C) (Carlson et al. 2014) and as a whole, tended to occur in shallower water (mid-Atlantic Bight and higher latitudes) (Rulifson & Moore 2009, Rulifson et al. 2012), which has been attributed to a higher thermal preference in southern groups rather than an inability to access deeper, cooler, offshore depths (Carlson et al. 2014). Carlson et al. (2014) concluded that the observed differences between the 2 tagged groups are not indicative of a migration pattern associated with a single coast-wide population of a large-scale migratory species.

Furthermore, in North and South Carolina, the maximum temperature of capture for *S. acanthias* has been reported as high as 24–29.1°C (Ulrich et al. 2007, Bangley & Rulifson 2017). The presence of active *S. acanthias* at temperatures >24°C contrasts evidence for estimated critical temperature limits in this study, and maximum temperatures of capture for northern *S. acanthias* groups (e.g. Jensen 1966, Castro 1983, McMillan & Morse 1999, Stehlik 2007, Bockus et al. 2020). Considering the timing and location of animal collections in this study compared to tagging studies, our samples are most likely to be representative of northern individuals. Such evidence suggests varying thermal tolerance across the latitudinal range of *S. acanthias*. However, the degree of difference in thermal tolerance between subpopulations, if any, is unclear, as is the mechanism driving such potential differences.

5. CONCLUSIONS

For *Squalus acanthias* in this study, 23°C likely represents an acute sublethal thermal tolerance limit, with mortality occurring at higher temperatures. However, loss of equilibrium occurred at temperatures as low as ~20°C, suggesting that population limits may occur well below the estimated critical temperature. We found no decrement in aerobic scope or α up to 23°C, suggesting that oxygen limitation does not adequately explain thermal limitation in this population, nor does aerobic scope indicate 'thermal optimality', sublethal thermal limits, or viable thermal habitat for this population. Future studies with this species should focus on identifying the primary drivers of thermal tolerance under varied environmental scenarios, acclimation to confirm thermal tolerance across longer time scales, and how thermal tolerance may vary with life stage, reproductive status, size, and across potential latitudinally divergent subpopulations. Such investigations may tease apart the current and long-term ability of *S. acanthias* to cope with a changing thermal environment across their extensive distribution and allow for better predictions of ecosystem consequences of shifting habitat viability.

Acknowledgements. This work was completed as part of A.M.A.'s PhD dissertation at the University of South Florida. We thank our contributors, Captain K. Wark for animal collection; L. Baskin and the Marine and Science Technology Academy students for their assistance in animal husbandry and treatment; Dr. H. Paluch for medical assessment; S. Hazlett, M. Mathes, L. Rodrigues-Mendoza, G. Chung, and A. Burns for assistance in husbandry and data collection; S. Hylton and H. Verkamp for insight and identification of dogfish reproductive status. We also thank C. T. Shaw for logistical planning and support and M. Birk and A. Timpe for physiological insights and discussion of metabolic calculations. We also thank the NOAA James J. Howard Laboratory personnel for support and assistance throughout the study, and our sources of funding, National Ocean and Atmospheric Administration OAR-COCA (#NA17OAR4310081) and the National Science Foundation (OCE-1419323 and OCE-1458967).

LITERATURE CITED

Angiletta MJ (2009) Thermal adaptation, a theoretical and empirical synthesis. Oxford University Press, New York, NY

ASMFC (Atlantic States Marine Fisheries Commission) (2002) Interstate fishery management plan for spiny dogfish. Fishery Management Report No. 40. Atlantic States Marine Fisheries Commission, Arlington, VA

Auer SK, Agreda E, Chen AH, Irshad M, Solowey J (2021) Late-stage pregnancy reduces upper thermal tolerance in a live-bearing fish. J Therm Biol 99:103022

Baeza J, Ferńandez M (2002) Active brood care in *Cancer setosus* (Crustacea: Decapoda): the relationship between female behaviour, embryo oxygen consumption and the cost of brooding. Funct Ecol 16:241–251

Bangley CW, Rulifson RA (2017) Habitat partitioning and diurnal nocturnal transition in the elasmobranch community of a North Carolina estuary. Bull Mar Sci 93: 319–338

Bartlett CB, Garber AF, Gonen S, Benfey TJ (2022) Acute critical thermal maximum does not predict chronic incremental thermal maximum in Atlantic salmon (*Salmo salar*). Comp Biochem Physiol A Mol Integr Physiol 266: 111143

Bates D, Maechler M, Bolker B, Walker S (2015) Fitting linear mixed-effects models using lme4. J Stat Softw 67: 1–48

Baty F, Ritz C, Charles S, Brutsche M, Flandrois J, Delignette-Muller M (2015) A toolbox for nonlinear regression in R: the package nlstools. J Stat Softw 66:1–21

Beitinger TL, Lutterschmidt WI (2011) Measures of thermal tolerance. In: Farrell AP (ed) Encyclopedia of fish physiology: from genome to environment. Academic Press, San Diego, CA, p 1695–1702

Benetti DD, Iversen ES, Ostrowski AC (1995) Growth rates of captive dolphin, *Coryphaena hippurus*, in Hawaii. Fish Bull 93:152–157

Bernal D, Donley JM, Shadwick RE, Syme DA (2005) Mammal-like muscles power swimming in a cold-water shark. Nature 437:1349–1352

Birk MA (2021) respirometry: Tools for conducting and analyzing respirometry experiments. R package version 1.3.0. https://CRAN.R-project.org/package=respirometry

Bockus AB, LaBreck CJ, Camberg JL, Collie JS, Seibel BA (2020) Thermal range and physiological tolerance mechanisms in two shark species from the Northwest Atlantic. Biol Bull (Woods Hole) 238:131–144

Borowiec BG, Crans KD, Khajali F, Pranckevicius NA, Young A, Scott GR (2016) Interspecific and environment-induced variation in hypoxia tolerance in sunfish. Comp Biochem Physiol A Mol Integr Physiol 198:59–71

Borowiec BG, Hoffman RD, Hess CD, Galvez F, Scott GR (2020) Interspecific variation in hypoxia tolerance and hypoxia acclimation responses in killifish from the family Fundulidae. J Exp Biol 223:jeb209692

Bouyoucos IA, Simpfendorfer CA, Planes S, Schwieterman GD, Weideli OC, Rummer JL (2022) Thermally insensitive physiological performance allows neonatal sharks to use coastal habitats as nursery areas. Mar Ecol Prog Ser 682:137–152

Brauner CJ, Richards JG (2020) Physiological performance in aquaculture: using physiology to help define optimal conditions for growth and environmental tolerance. Fish Physiol 38:83–121

Burgess G (2002) Spiny dogfish *Squalus acanthias* Linaeus 1758. In: Collette BB, Klein-MacPhee G (ed) Bigelow and Schroeder's fishes of the Gulf of Maine, 3rd edn. Smithsonian Institution Press, Washington, DC, p 54–57

Burton DT (1979) Ventilation frequency compensation responses of three eurythermal estuarine fish exposed to moderate temperature increases. J Fish Biol 15: 589–600

Caesar L, Rahmstorf S, Robinson A, Feulner G, Saba V (2018) Observed fingerprint of a weakening Atlantic Ocean overturning circulation. Nature 556:191–196

Campana S (2010) Tagging studies. In: Proceedings of the Transboundary Resources Assessment Committee (TRAC): spiny dogfish review. Transboundary Resources Assessment Committee, Woods Hole, MA, p 17–19

Campana SE, Gibson AJF, Marks L, Joyce W, Rulifson R, Dadswell M (2008) Stock structure, life history, fishery and abundance indices for spiny dogfish (*Squalus acanthias*) in Atlantic Canada. Can Sci Advis Sec Res Doc 2007/089

Campana SE, Kulka DW, Joyce S (2009) Growth and reproduction of spiny dogfish off the eastern coast of Canada, including inferences on stock structure. In: Gallucci VF, McFarlane GA, Bargmann GG (eds) Biology and management of dogfish sharks. American Fisheries Society, Bethesda, MD, p 195–208

Carlson AE, Hoffmayer ER, Tribuzio CA, Sulikowski JA (2014) The use of satellite tags to redefine movement patterns of spiny dogfish (*Squalus acanthias*) along the US east coast: implications for fisheries management. PLOS ONE 9:e103384

Castro JI (1983) The sharks of North American waters. Texas A&M University Press, College Station, TX

Castro JI, Peebles DR (2011) Spiny dogfish. In: The sharks of North America. Oxford University Press, Oxford, p 55–62

Chabot D, McKenzie DJ, Craig JF (2016a) Metabolic rate in fishes: definitions, methods and significance for conservation physiology. J Fish Biol 88:1–9

Chabot D, Steffensen JF, Farrell AP (2016b) The determination of standard metabolic rate in fishes. J Fish Biol 88: 81–121

Claireaux G, Chabot D (2016) Responses by fishes to environmental hypoxia: integration through Fry's concept of aerobic metabolic scope. J Fish Biol 88: 232–251

Clark TD, Sandblom E, Cox GK, Hinch SG, Farrell AP (2008) Circulatory limits to oxygen supply during an acute temperature increase in the Chinook salmon (*Oncorhynchus tshawytscha*). Am J Physiol Regul Integr Comp Physiol 295:R1631–R1639

Clark TD, Sandblom E, Jutfelt F (2013) Aerobic scope measurements of fishes in an era of climate change: respirometry, relevance and recommendations. J Exp Biol 216: 2771–2782

Clarke A (2006) Temperature and the metabolic theory of ecology. Funct Ecol 20:405–412

Clarke A, Fraser KPP (2004) Why does metabolism scale with temperature? Funct Ecol 18:243–251

Clarke A, Johnston N (1999) Scaling of metabolic rate with body mass and temperature in teleost fish. J Anim Ecol 68:893–905

Colvocoresses JA, Musick JA (1980) A preliminary evaluation of the potential for a shark fishery in Virginia. Special Report in Applied Marine Science and Ocean Engineering No. 234. Virginia Institute of Marine Science, Gloucester Point, VA.

Compagno LJV (1984) Food and agriculture organization species catalogue, Vol 4: sharks of the world—an annotated and illustrated catalogue of shark species known to date. FAO Fish Synop 125:251–655

Compagno L, Dando M, Fowler S (2005) Sharks of the world. Princeton University Press, Princeton, NJ

Dahlke FT, Wohlrab S, Butzin M, Pörtner HO (2020b) Thermal bottlenecks in the life cycle define climate vulnerability of fish. Science 369:65–70

Davis MW (2010) Fish stress and mortality can be predicted using reflex impairment. Fish Fish 11:1–11

Delignette-Muller ML, Dutang C (2015) fitdistrplus: an R package for fitting distributions. J Stat Softw 64:1–34

Dell'Apa A, Cudney-Burch J, Kimmel DG, Rulifson RA (2014) Sexual segregation of spiny dogfish in fishery-dependent surveys in Cape Cod, Massachusetts: potential management benefits. Trans Am Fish Soc 143: 833–844

Dell'Apa A, Bangley CW, Rulifson RA (2015) Who let the dogfish out? A review of management and socio-economic aspects of spiny dogfish fisheries. Rev Fish Biol Fish 25:273–295

Demirhan SA, Seyhan K (2006) Seasonality of reproduction and embryonic growth of spiny dogfish (*Squalus acanthias* L., 1758) in the eastern Black Sea. Turk J Zoo 30: 433–443

Deutsch C, Ferrel A, Seibel B, Pörtner HO, Huey RB (2015) Climate change tightens a metabolic constraint on marine habitats. Science 348:1132–1135

Deutsch C, Penn JL, Seibel B (2020) Metabolic trait diversity shapes marine biogeography. Nature 585:557–562

Diaz RJ, Breitburg DL (2009) The hypoxic environment. Fish Physiol 27:1–23

Diaz RJ, Rosenberg R (2008) Spreading dead zones and consequences for marine ecosystems. Science 321: 926–929

Dygert PH, Gunderson DR (1991) Energy utilization by embryos during gestation in viviparous copper rockfish, *Sebastes caurinus*. Environ Biol Fish 30:165–171

Easterling DR, Meehl GA, Parmesan C, Changnon SA, Karl TR, Mearns LO (2000) Climate extremes: observations, modeling, and impacts. Science 289: 2068–2074

Ege R, Krogh A (1914) On the relation between the temperature and the respiratory exchange in fishes. Int Rev Gesamten Hydrobiol Hydrograph 7:48–55

Eliason EJ, Clark TD, Hague MJ, Hanson LM and others (2011) Differences in thermal tolerance among sockeye salmon populations. Science 332:109–112

Elliott JM, Elliott JA (2010) Temperature requirements of Atlantic salmon *Salmo salar*, brown trout *Salmo trutta* and Arctic charr *Salvelinus alpinus*: predicting the effects of climate change. J Fish Biol 77:1793–1817

Elzhov TV, Mullen KM, Spiess AN, Bolker B (2016) minpack.lm: R interface to the Levenberg-Marquardt nonlinear least-squares algorithm found in MINPACL, plus support for bounds. R package version 1.2-1. https://CRAN.R-project.org/package=minpack.lm

Ern R, Huong DTT, Phuong NT, Madsen PT, Wang T, Bayley M (2015) Some like it hot: thermal tolerance and oxygen supply capacity in two eurythermal crustaceans. Sci Rep 5:10743

Ern R, Norin T, Gamperl AK, Esbaugh AJ (2016) Oxygen dependence of upper thermal limits in fishes. J Exp Biol 219:3376–3383

Farrell AP (2002) Cardiorespiratory performance in salmonids during exercise at high temperature: insights into cardiovascular design limitations in fishes. Comp Biochem Physiol A Mol Integr Physiol 132:797–810

Farrell AP, Hinch SG, Cooke SJ, Patterson DA, Crossin GT, Lapointe M, Mathes MT (2008) Pacific salmon in hot water: applying aerobic scope models and biotelemetry to predict the success of spawning migrations. Physiol Biochem Zool 81:697–708

Farrell ER, Boustany AM, Halpin PN, Hammond DL (2014) Dolphinfish (*Coryphaena hippurus*) distribution in relation to biophysical ocean conditions in the northwest Atlantic. Fish Res 151:177–190

Ferry-Graham LA, Gibb AC (2001) Comparison of fasting and postfeeding metabolic rates in a sedentary shark, *Cephaloscyllium ventriosum*. Copeia 2001:1108–1113

Ford D (1921) A contribution to our knowledge of the life histories of the dogfishes landed at Plymouth. J Mar Biol Assoc UK 12:468–505

Forsyth J, Andres M, Gawarkiewicz GG (2015) Recent accelerated warming of the continental shelf off New Jersey: observations from the CMV Oleander expendable bathythermograph line. J Geophys Res C Oceans 120: 2370–2384

Fox RJ, Donelson JM, Schunter C, Ravasi T, Gaitán-Espitia JD (2019) Beyond buying time: the role of plasticity in phenotypic adaptation to rapid environmental change. Philos Trans R Soc B 374:20180174

Friedland KD, Hare JA (2007) Long-term trends and regime shift in sea surface temperature on the continental shelf of the northeast United States. Cont Shelf Res 27: 2313–2328

Frölicher TL, Fischer EM, Gruber N (2018) Marine heatwaves under global warming. Nature 560:360–364

Frossard J, Renaud O (2021) Permutation tests for regression, ANOVA, and comparison of signals: the permuco package. J Stat Softw 99:1–32

Fry FEJ (1947) Effects of the environment on animal activity. Publ Ont Fish Res Lab 68:1–62

Fry FEJ (1971) The effect of environmental factors on the physiology of fish. Fish Physiol 6:1–98

Gienapp P, Teplitsky C, Alho J, Mills J, Merilä J (2008) Climate change and evolution: disentangling environmental and genetic responses. Mol Ecol 17:167–178

Gillooly JF, Brown JF, West GB, Savage VM, Charnov EL (2001) Effects of size and temperature on metabolic rate. Science 293:2248–2251

Gräns A, Jutfelt F, Sandblom E, Jönsson E and others (2014) Aerobic scope fails to explain the detrimental effects on growth resulting from warming and elevated CO_2 in Atlantic halibut. J Exp Biol 217:711–717

Green BS, McCormick MI (2005) O_2 replenishment to fish nests: males adjust brood care to ambient conditions and brood development. Behav Ecol 16:389–397

Großelindemann H, Ryan S, Ummenhofer CC, Martin T, Biastoch A (2022) Marine heatwaves and their depth structures on the Northeast US continental shelf. Front Clim 4:857937

Hammond D (2008) Using pop-off satellite archival tags to monitor and track dolphinfish and cobia. Cooperative Science Services, Charleston, SC

Hanchet S (1988) Reproductive biology of *Squalus acanthias* from the east coast, South Island, New Zealand. NZ J Mar Freshw Res 22:537–549

Harris JE (1952) A note on the breeding season, sex ratio and embryonic development of the dogfish *Scyliorhinus canicula* (L.). J Mar Biol Assoc UK 31:269–275

Hazen EL, Jorgensen S, Rykaczewski RR, Bograd SJ and others (2013) Predicted habitat shifts of Pacific top predators in a changing climate. Nat Clim Chang 3:234–238

Healy TM, Schulte PM (2012) Thermal acclimation is not necessary to maintain a wide thermal breadth of aerobic scope in the common killifish (*Fundulus heteroclitus*). Physiol Biochem Zool 85:107–119

Heuer RM, Stieglitz JD, Pasparakis C, Enochs IC, Benetti DD, Grosell M (2021) The effects of temperature acclimation on swimming performance in the pelagic mahi-mahi (*Coryphaena hippurus*). Front Mar Sci 8:654276

Hight BV, Lowe CG (2007) Elevated body temperatures of adult female leopard sharks, *Triakis semifasciata*, while aggregating in shallow nearshore embayments: Evidence for behavioral thermoregulation? J Exp Mar Biol Ecol 352:114–128

Hisaw FL, Albert A (1947) Observations on the reproduction of the spiny dogfish, *Squalus acanthias.* Biol Bull (Woods Hole) 92:187–199

Hobday AJ, Alexander LV, Perkins SE, Smale DA and others (2016) A hierarchical approach to defining marine heatwaves. Prog Oceanogr 141:227–238

Holder PE, Griffin LP, Adams AJ, Danylchuk AJ, Cooke SJ, Brownscombe JW (2020) Stress, predators, and survival: exploring permit (*Trachinotus falcatus*) catch-and-release fishing mortality in the Florida Keys. J Exp Mar Biol Ecol 524:151289

Huey RB, Kingsolver JG (2011) Variation in universal temperature dependence of biological rates. Proc Natl Acad Sci USA 108:10377–10378

IPCC (2019) IPCC special report on the ocean and cryosphere in a changing climate. Intergovernmental Panel on Climate Change, Geneva

Jensen AC (1966) Life history of the spiny dogfish. Fish Bull 65:527–554

Jewett EB, Eldridge PM, Burke MK, Buxton HT and others (2010) Scientific assessment of hypoxia in US coastal waters. Interim Report. Interagency Working Group on Harmful Algal Blooms, Hypoxia, and Human Health of the Joint Subcommittee on Ocean Science and Technology, Washington, DC

Jirik KE, Lowe CG (2012) An elasmobranch maternity ward: female round stingrays *Urobatis halleri* use warm, restored estuarine habitat during gestation. J Fish Biol 80:1227–1245

Johansen JL, Nadler LE, Habary A, Bowden AJ, Rummer J (2021) Thermal acclimation of tropical coral reef fishes to global heat waves. eLife 10:1–29

Johnston IA, Dunn J (1987) Temperature acclimation and metabolism in ectotherms with particular reference to teleost fish. Symp Soc Exp Biol 41:67–93

Jutfelt F, Norin T, Ern R, Overgaard J, Wang T, McKenzie DJ (2018) Oxygen- and capacity-limited thermal tolerance: blurring ecology and physiology. J Exp Biol 221: jeb169615

Kavanaugh MT, Rheuban JE, Luis KMA, Doney SC (2017) Thirty-three years of ocean benthic warming along the US northeast continental shelf and slope: patterns, drivers, and ecological consequences. J Geophys Res Oceans 122:9399–9414

Killen SS, Norin T, Halsey LG (2017) Do method and species lifestyle affect measures of maximum metabolic rate in fishes? J Fish Biol 90:1037–1046

Killen SS, Christensen EA, Cortese D, Zavorka L and others (2021) Guidelines for reporting methods to estimate metabolic rates by aquatic intermittent-flow respirometry. J Exp Biol 224:jeb242522

Kleiber M (1932) Body size and metabolism. Hilgardia 6: 315–353

Kleisner KM, Fogarty MJ, McGee S, Hare JA, Moret S, Perretti CT, Saba VS (2017) Marine species distribution shifts on the US northeast continental shelf under continued ocean warming. Prog Oceanogr 153: 24–36

Kraffe E, Tremblay R, Belvin S, LeCoz JR, Marty Y, Guderley H (2008) Effect of reproduction on escape responses, metabolic rates and muscle mitochondrial properties in the scallop *Placopecten magellanicus.* Mar Biol 156: 25–38

Lefevre S (2016) Are global warming and ocean acidification conspiring against marine ectotherms? A meta-analysis of the respiratory effects of elevated temperature, high CO_2 and their interaction. Conserv Physiol 4:cow009

Link JS, Garrison LP (2002) Changes in piscivory associated with fishing induced changes to the finfish community on Georges Bank. Fish Res 55:71–86

Lutterschmidt WI, Hutchison VH (1997) The critical thermal maximum: history and critique. Can J Zool 75:1561–1574

Madeira D, Narciso L, Cabral H, Diniz M, Vinagre C (2012) Thermal tolerance of the crab *Pachygrapsus marmoratus*: intraspecific differences at a physiological (CTMax) and molecular level (Hsp70). Cell Stress Chaperones 17: 707–716

Masonjones HD (2001) The effect of social context and reproductive status on the metabolic rates of dwarf seahorses (*Hippocampus zosterae*). Comp Biochem Physiol A Mol Integr Physiol 129:541–555

McMillan DG, Morse WM (1999) Spiny dogfish, *Squalus acanthias*, life history and habitat characteristics. NOAA Tech Memo NMFS-NE-150. https://repository.library.noaa.gov/view/noaa/3155

Meehl GA, Tebaldi C (2004) More intense, more frequent, and longer lasting heat waves in the 21st century. Science 305:994–997

Merten W, Appeldoorn R, Hammond D (2014a) Movements of dolphinfish (*Coryphaena hippurus*) along the US east coast as determined through mark and recapture data. Fish Res 151:114–121

Merten W, Appeldoorn R, Rivera R, Hammond D (2014b) Diel vertical movements of adult male dolphinfish (*Coryphaena hippurus*) in the western central Atlantic as determined by use of pop-up satellite archival transmitters. Mar Biol 161:1823–1834

Moore TM (1998) Population characteristics of the spiny dogfish, *Squalus acanthias* Linnaeus, 1758, from geographically distinct locations in Atlantic Canada during the summer and fall of 1996. MSc thesis, Acadia University, Wolfville

Morgan AC, Sulikowski JA (2015) The role of spiny dogfish in the northeast United States continental shelf ecosystem: how it has changed over time and potential interspecific competition for resources. Fish Res 167:260–277

Morley JW, Selden RL, Latour RJ, Frölicher TL, Seagraves RJ, Pinsky ML (2018) Projecting shifts in thermal habitat for 686 species on the North American continental shelf. PLOS ONE 13:e0196127

Moustahfid H, Tyrrell MC, Link JS, Nye JA, Smith BE, Gamble RJ (2010) Functional feeding responses of piscivorous fishes from the northeast US continental shelf. Oecologia 163:1059–1067

Muñoz NJ, Farrell AP, Heath JW, Neff BD (2018) Hematocrit is associated with thermal tolerance and modulated by developmental temperature in juvenile Chinook salmon. Physiol Biochem Zool 91:757–762

Nammack MF, Musick JA, Colvocoresses JA (1985) Life history of spiny dogfish off the northeastern United States. Trans Am Fish Soc 114:367–376

NEFSC (Northeast Fisheries Science Center) (2006) Report of the 43rd Northeast Regional Stock Assessment Workshop (43rd SAW). Northeast Fish Sci Cent Ref Doc

06–14. National Marine Fisheries Service, Woods Hole, MA

Nguyen KDT, Morley SA, Lai CH, Clark MS, Tan KS, Bates AE, Peck LS (2011) Upper temperature limits of tropical marine ectotherms: global warming implications. PLOS ONE 6:e29340

Norin T, Malte H, Clark TD (2014) Aerobic scope does not predict the performance of a tropical eurythermal fish at elevated temperatures. J Exp Biol 217:244–251

Nosal AP, Caillat A, Kisfaludy EK, Royer MA, Wegner NC (2014) Aggregation behavior and seasonal philopatry in male and female leopard sharks *Triakis semifasciata* along the open coast of southern California, USA. Mar Ecol Prog Ser 499:157–175

Nye JA, Link JS, Hare JA, Overholtz WJ (2009) Changing spatial distribution of fish stocks in relation to climate and population size on the Northeast United States continental shelf. Mar Ecol Prog Ser 393:111–129

Oliver ECJ, Donat MG, Burrows MT, Moore PJ and others (2018) Longer and more frequent marine heatwaves over the past century. Nat Commun 9:1324

Oliver ECJ, Burrows MT, Donat MG, Sen Gupta A and others (2019) Projected marine heatwaves in the 21st century and the potential for ecological impact. Front Mar Sci 6:734

Oliver EC, Benthuysen JA, Darmaraki S, Donat MG and others (2021) Marine heatwaves. Annu Rev Mar Sci 13: 313–342

Palko BJ, Beardsley GL, Richards WJ (1982) Synopsis of the biological data on dolphin-fishes, *Coryphaena hippurus* Linnaeus and *Coryphaena equiselis* Linnaeus. https://repository.library.noaa.gov/view/noaa/5470/noaa_5470_DS1.pdf

Pawar S, Dell AI, Savage VM, Knies JL (2016) Real versus artificial variation in the thermal sensitivity of biological traits. Am Nat 187:E41–E52

Pecl GT, Araújo MB, Bell JD, Blanchard J and others (2017) Biodiversity redistribution under climate change: impacts on ecosystems and human well-being. Science 355: eaai9214

Pershing AJ, Alexander MA, Hernandez CM, Kerr LA and others (2015) Slow adaptation in the face of rapid warming leads to collapse of the Gulf of Maine cod fishery. Science 350:809–812

Pinsky ML, Worm B, Fogarty MJ, Sarmiento JL, Levin SA (2013) Marine taxa track local climate velocities. Science 341:1239–1242

Pistevos JC, Nagelkerken I, Rossi T, Olmos M, Connell SD (2015) Ocean acidification and global warming impair shark hunting behaviour and growth. Sci Rep 5: 16293

Pörtner HO (2010) Oxygen- and capacity-limitation of thermal tolerance: a matrix for integrating climate related stressor effects in marine ecosystems. J Exp Biol 213: 881–893

Pörtner HO, Knust R (2007) Climate change affects marine fishes through the oxygen limitation of thermal tolerance. Science 315:95–97

Precht H (1958) Concepts of the temperature adaptation of unchanging reaction systems of cold-blooded animals. In: Prosser CL (ed) Physiological adaptation. American Physiological Society, Washington, DC, p 50–78

Prosser CL (ed) (1991) Comparative animal physiology, environmental and metabolic animal physiology. John Wiley & Sons, Hoboken, NJ

Prosser CL, Nelson DO (1981) The role of nervous systems in temperature adaptation of poikilotherms. Annu Rev Physiol 43:281–300

R Core Team (2017) R: a language and environment for statistical computing. R Foundation for Statistical Computing, Vienna

R Core Team (2020) R: a language and environment for statistical computing. R Foundation for Statistical Computing, Vienna

Raby GD, Donaldson MR, Hinch SG, Patterson DA and others (2012) Validation of reflex indicators for measuring vitality and predicting the delayed mortality of wild coho salmon bycatch released from fishing gears. J Appl Ecol 49:90–98

Rafferty AR, Brazer EO Jr, Reina RD (2012) Depredation by harbor seal and spiny dogfish in a Georges Bank gillnet fishery. Fish Manag Ecol 19:264–272

Rago PJ, Sosebee KA, Brodziak JKT, Murawski SA, Anderson ED (1998) Implications of recent increases in catches on the dynamics of Northwest Atlantic spiny dogfish (*Squalus acanthias*). Fish Res 39:165–181

Rahmstorf S, Coumou D (2011) Increase of extreme events in a warming world. Proc Natl Acad Sci USA 108: 17905–17909

Reusch TB (2014) Climate change in the oceans: evolutionary versus phenotypically plastic responses of marine animals and plants. Evol Appl 7:104–122

Richter K, Haslbeck M, Buchner J (2010) The heat shock response: life on the verge of death. Mol Cell 40: 253–266

Rogers NJ, Urbina MA, Reardon E, McKenzie DJ, Wilson RW (2016) A new analysis of hypoxia tolerance in fishes using a database of critical oxygen level (P_{crit}). Conserv Physiol 4:cow012

Rogers AD, Frinault BAV, Barnes DKA, Bindoff NL and others (2020) Antarctic futures: an assessment of climate-driven changes in ecosystem structure, function, and service provisioning in the Southern Ocean. Annu Rev Mar Sci 12:87–120

Rubalcaba JG, Verberk WC, Hendriks AJ, Saris B, Woods HA (2020) Oxygen limitation may affect the temperature and size dependence of metabolism in aquatic ectotherms. Proc Natl Acad Sci USA 117:31963–31968

Rulifson RA (2010) Tagging spiny dogfish overwintering in North Carolina, and summering in Bay of Fundy, Canada. In: Proceedings of the Transboundary Resources Assessment Committee (TRAC): spiny dogfish review. Transboundary Resources Assessment Committee, Woods Hole, MA, p 15–17

Rulifson RA, Moore TM (2009) Population estimates of spiny dogfish aggregations overwintering south of Cape Hatteras, North Carolina, using an area density method. In: Gallucci VF, McFarlane GA, Bargmann GG (eds) Biology and management of dogfish sharks. American Fisheries Society, Bethesda, MD, p 133–138

Rulifson RA, Cudney-Burch JE, Hemilright D (2012) Coastal movements of spiny dogfish overwintering off the Outer Banks, NC. North Carolina Sea Grant Fisheries Resource Grant Program completion report, Grant number 08–FEG-11. North Carolina State University, Raleigh, NC

Rulifson RA, Pratt M, Bell TJ, Parente I, Cudney-Burch J, Dell'Apa A (2012a) Is Cape Cod a natural delineation for migratory patterns in US and Canadian spiny dogfish stocks? Final Report for the Commercial Fisheries

Research Foundation. Southern New England Collaborative Research Initiative, Saunderstown, RI

Rummer JL, Binning SA, Roche DG, Johansen JL (2016) Methods matter: considering locomotory mode and respirometry technique when estimating metabolic rates of fishes. Conserv Physiol 4:cow008

Ryan S, Ummenhofer CC, Gawarkiewicz G, Wagner P, Scheinert M, Biastoch A, Böning CW (2021) Depth structure of Ningaloo Niño/Niña events and associated drivers. J Clim 34:1767–1788

Saba VS, Griffies SM, Anderson WG, Winton M and others (2016) Enhanced warming of the Northwest Atlantic Ocean under climate change. J Geophys Res Oceans 121: 118–132

Sagarese SR, Frisk MG, Cerrato RM, Sosebee KA, Musick JA, Rago PJ (2014) Application of generalized additive models to examine ontogenetic and seasonal distributions of spiny dogfish (*Squalus acanthias*) in the northeast (US) shelf large marine ecosystem. Can J Fish Aquat Sci 71:847–877

Sandblom E, Gräns A, Axelsson M, Seth H (2014) Temperature acclimation rate of aerobic scope and feeding metabolism in fishes: implications in a thermally extreme future. Proc R Soc B 281:20141490

Scheffers BR, De Meester L, Bridge TC, Hoffmann A and others (2016) The broad footprint of climate change from genes to biomes to people. Science 354:aaf7671

Schlegel RW, Oliver EC, Chen K (2021) Drivers of marine heatwaves in the Northwest Atlantic: the role of air–sea interaction during onset and decline. Front Mar Sci 8: 627970

Schulte PM (2015) The effects of temperature on aerobic metabolism: towards a mechanistic understanding of the responses of ectotherms to a changing environment. J Exp Biol 218:1856–1866

Schulte PM, Healy TM, Fangue NA (2011) Thermal performance curves, phenotypic plasticity, and the time scales of temperature exposure. Integr Comp Biol 51: 691–702

Seebacher F, Franklin CE (2012) Determining environmental causes of biological effects: the need for a mechanistic physiological dimension in conservation biology. Philos Trans R Soc B 367:1607–1614

Seibel BA, Birk MA (2022) Unique thermal sensitivity imposes a cold-water energetic barrier for vertical migrators. Nat Clim Chang 12:1052–1058

Seibel BA, Deutsch C (2020) Oxygen supply capacity in animals evolves to meet maximum demand at the current oxygen partial pressure regardless of size or temperature. J Exp Biol 223:jeb210492

Seibel BA, Andres A, Birk MA, Burns AL, Shaw CT, Timpe AW, Welsh CJ (2021) Oxygen supply capacity breathes new life into critical oxygen partial pressure (P_{crit}). J Exp Biol 224:jeb242210

Selden RL, Batt RD, Saba VS, Pinsky ML (2018) Diversity in thermal affinity among key piscivores buffers impacts of ocean warming on predator–prey interactions. Glob Change Biol 24:117–131

Shepherd T, Page F, Macdonald B (2002) Length and sex-specific associations between spiny dogfish (*Squalus acanthias*) and hydrographic variables in the Bay of Fundy and Scotian Shelf. Fish Oceanogr 11:78–89

Slesinger E, Andres A, Young R, Seibel B and others (2019) The effect of ocean warming on black sea bass (*Centropristis striata*) aerobic scope and hypoxia tolerance. PLOS ONE 14:e0218390

Slesinger E, duPontavice H, Seibel B, Saba VS, Kohut J, Saba GK (2024) Climate-induced reduction in metabolically suitable habitat for U.S. northeast shelf marine species. PLOS Clim 3:e0000357

Snyder S, Nadler LE, Bayley JS, Svendsen MBS, Johansen JL, Domenici P, Steffensen JF (2016) Effect of closed v. intermittent flow respirometry on hypoxia tolerance in the shiner perch *Cymatogaster aggregata.* J Fish Biol 88: 252–264

Sollid J, Nilsson GE (2006) Plasticity of respiratory structures — adaptive remodeling of fish gills induced by ambient oxygen and temperature. Respir Physiol Neurobiol 154:241–251

Somero GN (2022) The Goldilocks Principle: a unifying perspective on biochemical adaptation to abiotic stressors in the sea. Annu Rev Mar Sci 14:1–23

Speers-Roesch B, Mandic M, Groom DJ, Richards JG (2013) Critical oxygen tensions as predictors of hypoxia tolerance and tissue metabolic responses during hypoxia exposure in fishes. J Exp Mar Biol Ecol 449: 239–249

Stehlik LL (2007) Essential fish habitat source document: spiny dogfish, *Squalus acanthias*, life history and habitat characteristics, 2nd edn. NOAA Tech Memo NMFS-NE-203. https://repository.library.noaa.gov/view/noaa/3528/noaa_3528_DS1.pdf

Stocker TF, Qin D, Plattner GK, Tignor M and others (2013) Climate change 2013: the physical science basis. Contribution of Working Group I to the Fifth Assessment Report of the Intergovernmental Panel on Climate Change. Cambridge University Press, Cambridge

Svendsen MBS, Bushnell P, Steffensen JF (2016) Design and setup of intermittent flow respirometry system for aquatic organisms. J Fish Biol 88:26–50

Templeman W (1984) Migrations of spiny dogfish, *Squalus acanthias*, and recapture success from tagging in the Newfoundland area, 1963–65. J Northwest Atl Fish Sci 5: 47–53

Timmerman CM, Chapman LJ (2003) The effect of gestational state on oxygen consumption and response to hypoxia in the sailfin molly, *Poecilia latipinna.* Environ Biol Fishes 68:293–299

Ulrich GF, Jones CM, Driggers WB, Drymon JM, Oakley D, Riley C (2007) Habitat utilization, relative abundance, and seasonality of sharks in the estuarine and nearshore waters of South Carolina. Am Fish Soc Symp 50:125–139

Veríssimo A, McDowell JR, Graves JE (2010) Global population structure of the spiny dogfish *Squalus acanthias*, a temperate shark with an antitropical distribution. Mol Ecol 19:1651–1662

Veríssimo A, Grubbs D, McDowell J, Musick J, Portnoy D (2011) Frequency of multiple paternity in the spiny dogfish *Squalus acanthias* in the Western North Atlantic. J Hered 102:88–93

Wheeler CR, Kneebone J, Heinrich D, Strugnell JM, Mandelman JW, Rummer JL (2022) Diel rhythm and thermal independence of metabolic rate in a benthic shark. J Biol Rhythms 37:484–497

Whitney NM, Lear KO, Morris JJ, Hueter RE, Carlson JK, Marshall HM (2021) Connecting post-release mortality to the physiological stress response of large coastal sharks in a commercial longline fishery. PLOS ONE 16: e0255673

Wood CM (2018) The fallacy of the P_{crit}—Are there more useful alternatives? J Exp Biol 221:jeb163717

Wu L, Cai W, Zhang L, Nakamura H and others (2012) Enhanced warming over the global subtropical western boundary currents. Nat Clim Chang 2:161−166

Zanuzzo FS, Bailey JA, Garber AF, Gamperl AK (2019) The acute and incremental thermal tolerance of Atlantic cod (*Gadus morhua*) families under normoxia and mild hypoxia. Comp Biochem Physiol A Mol Integr Physiol 233: 30−38

Zhang J, Gilbert D, Gooday AJ, Levin L and others (2010) Natural and human-induced hypoxia and consequences for coastal areas: synthesis and future development. Biogeosciences 7:1443−1467

Editorial responsibility: Craig Radford,
Warkworth, New Zealand
Reviewed by: 3 anonymous referees

Submitted: July 6, 2023
Accepted: April 9, 2024
Proofs received from author(s): May 30, 2024